AD_____
(Leave blank)

Award Number: **W81XWH-07-1-0692**

TITLE: **LIV-1 and Zn transporters: establishing a link between hyperprolactinemia and breast cancer**

PRINCIPAL INVESTIGATOR: **Shannon L Kelleher, Ph.D.**

CONTRACTING ORGANIZATION: **Pennsylvania State University**
University Park, PA 16802

REPORT DATE: O**ctober 2008**

TYPE OF REPORT: **Final**

PREPARED FOR: U.S. Army Medical Research and Materiel Command
Fort Detrick, Maryland 21702-5012

DISTRIBUTION STATEMENT: (Check one)

X Approved for public release; distribution unlimited

☐ Distribution limited to U.S. Government agencies only; report contains proprietary information

The views, opinions and/or findings contained in this report are those of the author(s) and should not be construed as an official Department of the Army position, policy or decision unless so designated by other documentation.

REPORT DOCUMENTATION PAGE

Form Approved
OMB No. 0704-0188

1. REPORT DATE *(DD-MM-YYYY)*	2. REPORT TYPE	3. DATES COVERED *(From - To)*
14-10-2008	Final	15 Sep 2007-14 Sep 2008

4. TITLE AND SUBTITLE

LIV-1 and Zn transporters: establishing a link between hyperprolactinemia and breast cancer

5a. CONTRACT NUMBER
W81XWH-07-1-0692

5b. GRANT NUMBER
BC062742

5c. PROGRAM ELEMENT NUMBER

6. AUTHOR(S)
Shannon L Kelleher, Ph.D., Veronica Lopez

Email: jri1@psu.edu

5d. PROJECT NUMBER

5e. TASK NUMBER

5f. WORK UNIT NUMBER

7. PERFORMING ORGANIZATION NAME(S) AND ADDRESS(ES)

Pennsylvania State University
University Park, Pennsylvania
16802-1004

8. PERFORMING ORGANIZATION REPORT NUMBER

9. SPONSORING / MONITORING AGENCY NAME(S) AND ADDRESS(ES)

U.S. Army Medical Research and Materiel Command
Fort Detrick, Maryland 21702-5012

10. SPONSOR/MONITOR'S ACRONYM(S)

11. SPONSOR/MONITOR'S REPORT NUMBER(S)

12. DISTRIBUTION / AVAILABILITY STATEMENT

Approved for public release; distribution unlimited

13. SUPPLEMENTARY NOTES

14. ABSTRACT

Evidence implicates dysregulated cellular zinc (Zn) metabolism in breast cancer. Regulation of Zn transport controls programmed cell death which is uncoupled in cancer. A relationship between hyperprolactinemia and breast cancer has been observed. We speculate prolactin modulates cellular Zn metabolism. Clinical studies have suggested the Zn importer Zip6 (LIV-1) as a prognostic marker for breast cancer; however, the functional relevance is unknown. We explored Zip6 function and examined its regulation by prolactin in tumorigenic (T47D) cells. Zinc level of T47D cells was 20% higher than in normal breast cells. Zip6 protein abundance was ~10-fold higher, ~90% of which was located intracellularly, suggesting that if functional, Zip6 traffics to the plasma membrane. Zip6-attenuation reduced cellular Zn level, cytochrome c release and caspase activity but preliminarily increased cell proliferation and tumorigenesis potentially from decreased E-cadherin expression. Prolactin increased Zn uptake; however, neither Zip6 expression or localization was affected, implicating other Zn transporters in this process. In summary, Zip6 over-expression may act as a "tumor suppressor" suggesting that therapies attempting to attenuate Zip6 expression may result in enhanced proliferation and metastasis. Thus, elucidating novel prognostic markers and understanding their role in breast cancer transformation and progression is critical to developing efficacious therapies.

15. SUBJECT TERMS
zinc, breast cancer, Zip6, LIV1, mitochondria, apoptosis, prolactin

16. SECURITY CLASSIFICATION OF:			17. LIMITATION OF ABSTRACT	18. NUMBER OF PAGES	19a. NAME OF RESPONSIBLE PERSON
a. REPORT	b. ABSTRACT	c. THIS PAGE			19b. TELEPHONE NUMBER *(include area code)*
U	U	U	UU	57	USAMRMC

Table of Contents

	Page
Introduction……..	**4**
Body……..	**5- 20**
Key Research Accomplishments……..	**21**
Reportable Outcomes……	**22**
Conclusion……	**23**
References……	**24-25**
Appendices……	**26-28**
Supporting Data……..	**29-57**

Introduction

Breast cancer is one of the leading causes of death among women with ductal carcinomas representing ~30% of all diagnoses. The etiology of breast cancer is multifactorial and generally not understood; however, compelling evidence implicates dysregulated zinc (Zn) homeostasis in breast cancer cells. This significance of this lies in the fact that tight regulation of cellular Zn metabolism plays a regulatory role in modulating programmed cell death (apoptosis), a cellular process which is uncoupled in cancer. We speculate that alterations in Zn transporting mechanisms in breast cells dysregulates intrinsically mediated apoptogenic mechanisms. The Zn transporter Zip6 (LIV-1) imports Zn into the cell. Several studies have associated over-expression of Zip6 with breast cancer which we postulate may functionally link dysregulated Zn metabolism with aberrant cellular function. Currently the cellular consequences of Zip6 over-expression in breast cancer cells in not understood. Recently a relationship between elevated prolactin levels (hyperprolactinemia) and breast cancer has been observed. Clinical implications reflect the fact that drugs which are widely prescribed for treatment of a range of mental and neurodegenerative illnesses including Parkinson's and depression (e.g. dopamine antagonists) secondarily increase prolactin levels, potentially increasing breast cancer risk in an extraordinary number of individuals. Studies from our research group have determined that prolactin regulates numerous Zn transporters in normal breast cells thus we speculate that hyperprolactinemia may potentiate the dysregulation of Zn metabolism observed in breast cancer cells. The purpose of our research plan was three-fold; 1) to first determine the functional relevance of Zip6 over-expression in ductal tumorigenic breast carcinoma cells on intrinsic apoptogenic mechanisms; 2) to determine if prolactin modulates Zip6 expression or localization in ductal tumorigenic breast carcinoma cells; and 3) to screen for altered expression of other Zn transporting proteins in ductal tumorigenic breast carcinoma cells in hopes of identifying other Zn transporters which may facilitate the dysregulation of cellular Zn metabolism in breast cancer. The scope of our research plan utilized several cultured breast cell models. We first validated T47D cells as an appropriate model of ductal carcinoma to explore effects of Zip6 over-expression on cellular Zn pools and apoptogenic mechanisms. We genetically manipulated Zip6 expression and aimed to directly determine effects on intracellular Zn pools, cellular energetics (m-aconitase activity) and markers of intrinsic apoptosis including caspase activity, cytochrome c oxidase release from the mitochondria (the upstream modulator of caspase activity), and DNA fragmentation (the final product of apoptosis). Thirdly, we explored the potential of hyperprolactinemia to modulate Zip6 expression and cellular localization. Finally, we utilized a screen-based approach to identify Zn transporters other than Zip6 whose expression might be dysregulated in tumorigenic breast cancer cells in hopes of identifying further targets of exploration.

Project Summary: LIV-1(Zip6) and Zn transporters: establishing a link between hyperprolactinemia and breast cancer

Introduction

While little is known regarding the role of zinc (Zn) homeostasis in breast cancer, the dysregulation of cellular Zn metabolism has been implicated in carcinogenesis (1) . For example, elevated Zn concentrations were observed in chemically induced rat mammary tumors compared to normal tissues (2), similar to what has been shown in human breast cancer tissue (3,4). Cellular Zn homeostasis is coordinated through the functional activities of numerous Zn-specific transporters which are members of two distinct gene families. Members of the *SLC39A* gene family (ZRTL-like Import Proteins; Zip1-14) are responsible for Zn import into the cytoplasm, either across the plasma membrane or out of intracellular organelles (5). In contrast, members of the *SLC30A* gene family (ZnT1-10) export Zn from the cytoplasm, either across the plasma membrane into the extracellular space or for accumulation into intracellular organelles (5). Mounting evidence has associated dysregulation of Zn transporting proteins with the transition or progression of breast cancer. *With this in mind, Task 1 aimed to A) screen for differences in Zn transporter expression between tumorigenic and non-cancerous breast cells; and B) specifically explore the differential expression of Zip6 between tumorigenic and non-cancerous breast cells.* Compelling evidence suggests that the inability of cells to regulate intracellular Zn homeostasis may result in dysregulation of apoptogenic mechanisms and malignancy progression in breast cells (2,4). This postulate is evidenced by aberrant expression of proteins that are responsible for transporting Zn such as ZnT1, metallothionein (MT), and Zip6 in breast cancer cell lines and in human breast tumor biopsies (2,6-10). *With this in mind, Task 2 aimed to determine if Zn transported by the Zn importer Zip6 plays a role in dysregulation of apoptogenic mechanisms.* Finally, understanding the etiology of Zip6 over-expression and the regulation of Zip6 expression and localization may provide important therapeutic clues. Prolactin (PRL) is essential for mammary gland growth, differentiation and lactation (11,12). Several studies have described a direct correlation between hyperprolactinemia (hyperPRL; abnormally high systemic PRL level) and breast cancer; however, the significance of this relationship is unknown. Most studies have focused on the role of PRL in the regulation of cell signaling mechanisms directly associated with cell cycle control and apoptogenesis. We have previously determined that PRL plays a regulatory role in Zn homeostasis in normal mammary cells (13,14) and have shown that expression and localization of several Zn transporters in normal mammary cells is regulated at the transcription and post-translational level by PRL (14). For example, PRL stimulates the expression of Zip3 and the movement of Zip3 from an intracellular compartment to the plasma membrane thus increasing Zn uptake into the cell. *With this in mind, Task 3 aimed to explore the regulation of Zip6 expression and localization by PRL in tumorigenic T47D cells.* **Together, the studies outlined in this proposal explored the functional relevance of dysregulated expression of a specific Zn transporting mechanism (Zip6) which has been previously implicated as a possible prognostic marker in breast cancer. Towards this end we have generated intriguing preliminary data which suggests that Zip6 does regulate apoptogenesis; however, if expression is attenuated, tumorigenic cells may develop a metastatic phenotype. Secondly, we conducted an expression screen to compare expression of numerous other Zn transporters between tumorigenic and normal breast cells which**

have identified further important avenues of investigation. In particular, we have identified Zip8 and ZnT2 as exciting novel candidates to pursue in subsequent studies.

Task 1. To determine differences in zinc transporter expression and characterize the expression, protein abundance and localization of Zip6 in normal (HMEC and HC11) and tumorigenic (T47D) breast cells

A. Differential expression of Zn transporters in breast cancer cells

To first identify Zn transporting mechanisms which may play a role in the dysregulation of Zn homeostasis in breast cancer, real-time semi-quantitative-PCR (Q-PCR) was used to screen for differences in Zn transporter expression between tumorigenic (T47D) and normal (HME) human breast cells. We compared mRNA abundance of several Zn importers (Zip1, -3, -6, -8 and -10) and exporters (ZnT1, -2, and -4). Our data demonstrated that mRNA levels of Zip1, Zip8 and Zip10 were significantly higher (1.5-fold, 3-fold and 2-fold, respectively), in T47D cells whereas mRNA levels of Zip3 and Zip6 were significantly lower (2-fold) compared with mRNA abundance in HME cells (Figure 1A). With respect to Zn exporters, we determined that ZnT1 mRNA level was significantly higher (2-fold), whereas ZnT2 mRNA was virtually undetectable in T47D compared with HME cells (Figure 1B). The ability of cells to tightly regulate Zn import, export or accumulation is critical as subtle alterations in cellular Zn levels are known to regulate cell metabolism, including mitochondrial function and apoptosis (15,16). **Together these data identified numerous Zn transporter targets which will allow for the exploration of cellular mechanisms that may be responsible for the dysregulation of cellular Zn pools in tumorigenic breast cells. Based on these data, we speculate that over-expression of specific Zn importers in T47D cells such as Zip1, Zip8 and Zip10 may increase the vulnerability of breast cells excess Zn levels. Alternatively, the dysregulation of Zn transporters that play a role in Zn export or accumulation such as ZnT1 and ZnT2, respectively, may contribute to the inability of T47D cells to properly protect themselves from excess Zn.**

B. Characterization of Zip6 expression and localization in T47D cells

Our studies are not the first to identify dysregulated Zn transporter expression in breast cancer cells. Interestingly, expression of the Zn importer, Zip6 (LIV-1), has been shown to be stimulated by estrogen in breast cancer cell lines (17) and Zip6 expression is significantly correlated with the spread of breast cancer to the lymph nodes (18). Somewhat counter intuitively, studies have detected a negative correlation between Zip6 protein abundance and tumor size, grade and stage, which implicates high Zip6 protein levels with less aggressive tumors (19). Further controversy arises with respect to the localization of Zip6 within the cell. Although over-expression of human Zip6 in transfected CHO cells increases Zn uptake (18), studies exploring the localization of endogenous Zip6 in breast cancer biopsies have demonstrated that abundant Zip6 is localized intracellularly (19). As a result of studies such as these, Zip6 has been suggested to be a prognostic marker for breast cancer; however, the mechanistic and pathophysiological relevance of dysregulated Zip6 expression and perhaps localization and moreover, how it relates to breast cell function and breast cancer transformation or progression is not understood. Thus, our second objective was to characterize the expression and localization of Zip6 in a tumorigenic breast cancer cell line (T47D) with the long-term goal of using it as a model to explore the role of Zip6 in modulating intracellular Zn pools and evalutating cell function. We first determined the relative expression of Zip6 in human T47D cells, normal human (HME) and mouse (HC11) breast cells relative to a control gene (β-actin). Our data demonstrated that both human cell lines, (HME and T47D), abundantly expressed Zip6 mRNA relative to β-actin (~145% and ~92% higher, respectively) (Figure 2A). Further analysis revealed that Zip6 mRNA abundance in T47D cells was significantly lower (~40%) compared

with HME cells (Figure 2A), mirroring observations from breast cancer biopsies. Much of our research utilizes a normal mouse breast cell line (HC11) which expresses both prolactin and estrogen receptors. To determine whether HC11 cells could be used for further studies outlined within this proposal, we analyzed Zip6 mRNA abundance by Q-PCR. As can be gleaned from Figure 2B, while Zip6 mRNA was detected in HC11 cells, Zip6 abundance was only slightly higher (~15%) relative to the expression of β-actin and ~100-fold lower than what we detected in HME cells (Figure 2B), suggesting that HC11 cells may not be a good model for exploring the regulation and function of Zip6 due to the lack of similarity to human cell lines. In contrast to the difference in mRNA abundance, we determined that Zip6 protein abundance was significantly higher in T47D cells compared with HME cells (Figure 2A, inset) by immunoblotting using a Zip6 antibody that was a gift from Dr. Liping Huang (USDA/UC Davis). This demonstrated that an inverse relationship between Zip6 mRNA and protein abundance exists in T47D cells which has also been observed in human breast cancer biopsies (18) thereby validating T47D cells as an appropriate human tumorigenic cell model for our proposal. A critical point to note is that while Zip6 protein was detected in HME cells, Zip6 protein could not be detected in HC11 cells despite the fact that the epitope the antibody was generated against was homolgous in human and mouse (Figure 2B, inset). Thus this observation eliminated the use of HC11 cells as an appropriate model of normal breast cells to explore the functional analysis of Zip6 as proposed in our initial project outline.

As mentioned previously, the sub-cellular localization of Zip6 has not been well characterized. While Zip6 is expressed on the cell surface in a transfected cell model, another report has suggested that endogenous Zip6 can be detected at the plasma membrane and in an intracellular compartment in breast cancer biopsies (19). Therefore, we next conducted an exhaustive series of sub-cellular co-localization studies of endogenous Zip6 in T47D cells with the aim of determining where Zip6 is localized in hopes of comparing its localization in normal HME cells. To determine if Zip6 is associated with the plasma membrane in our breast cell models, localization was first visualized by confocal microscopy. Figure 3 illustrates that Zip6 was localized exo-facially in both HME (Figure 3A, B) and T47D cells (Figure 3C, D) using non-permeabilized conditions (without 0.2% TritonX-100). To confirm that Zip6 was associated directly with the plasma membrane, cell membrane-associated proteins were biotinylated then affinity separated from non-biotinylated intracellular membranes using avidinated beads. Membrane proteins were separated by electrophoresis and plasma membrane-associated (biotinylated) and intracellular membrane-associated (non-biotinylated) Zip6 was detected by immunoblotting. Interestingly, our data clearly demonstrated that in sharp contrast to the exclusive localization of Zip6 associated with the plasma membrane in normal HME cells, ~90% of Zip6 protein was localized intracellularly in tumorigenic T47D cells (Figure 4). These data are the first to clearly document specific intracellular localization of the Zn importer Zip6 in breast cancer cells. Based on these data, we next utilized confocal microscopy to attempt to identify the intracellular compartment(s) which Zip6 is associated with as our results indicated that Zip6 is not only over-expressed but may be mis-localized in tumorigenic T47D cells. Intriguingly, Zip6 was observed in a unique and discrete spindle-like intracellular compartment in T47D cells (Figure 5). The identification of this compartment is of particular interest as abnormal protein localization is often linked to metabolic cellular disorders. In an attempt to identify the aberrant sub-cellular localization of endogenous Zip6 in breast cancer cells, we separated sub-cellular fractions by differential centrifugation. These sub-cellular fractions were further separated by electrophoresis then immunoblotted for Zip6. Differential centrifugation of proteins from tumorigenic T47D cells revealed that Zip6 protein was associated with the more dense cellular organelles such as the nucleus (N) and heavy mitochondria (Hm) fractions, with minimal expression in fractions containing lysosome and smaller cytoplasmic proteins (Figure 6). The detection of Zip6 in fractions containing mitochondria was particularly intriguing, thus

we isolated mitochondria and rigorously digested non-mitochondrial proteins with proteinase K. As illustrated in Figure 7, we were unable to detect Zip6 in purified mitochondrial fractions. We next utilized confocal microscopy in an attempt to localize Zip6 with a specific intracellular compartment(s). As illustrated in Figure 8, immunofluorescent imaging eliminated the nucleus (TOPRO-3), endoplasmic reticulum (calnexin), and mitochondria (CoxIV) as sub-cellular compartments that Zip6 is associated with (Figure 8A-D). **Taken together these data indicate that similar to reports by others (19), Zip6 mRNA and protein levels are inversely related in tumorigenic T47D cells suggesting that T47D cells may be a useful model for exploring the functional consequences of dysregulated Zip6 function in breast cancer. Our results suggest that low Zip6 mRNA level may actually reflect down-regulation response to excessive Zip6 protein abundance which may result in increased Zn uptake into breast tumor cells. Studies remain underway to determine the unique sub-cellular localization of endogenous Zip6 in tumorigenic T47D cells and to determine if Zip6 can traffic to the plasma membrane to functionally import Zn. These studies are outside the scope of this proposal.**

Generation and characterization of Zip6 antibody

Our initial work examining Zip6 protein abundance *(above)* was performed using a small aliquot of Zip6 antibody generously provided by Dr. Liping Huang, as antibody to Zip6 is not commercially available. We therefore contracted with Genemed Synthesis (San Antonio, TX) to produce rabbit polyclonal antibodies against the identical Zip6 peptide sequence used by Dr. Huang (VSEPRKSFMYSRNTNDN) (20) as we had successfully used this method and this company for the production of over 20 over custom peptide antibodies. Once we received our rabbit antiserum, we aimed to validate our antibody. To validate the specificity of our newly produced Zip6 antibody, we isolated crude membrane fractions from tumorigenic T47D cells, separated them by electrophoresis and immunoblotted for Zip6. As shown in Figure 9A, we were able to identify a single major band at ~50 kDa which was completely eliminated by peptide competition (Figure 9B). This clearly indicated that the antibody immunoreacted against the peptide. However, the antibody provided by Dr. Huang detected a single major band at ~75 kDa (Figure 9C) similar the predicted molecular mass and to previous published reports (18,20). We then used immunoaffinity chromatography to purify our Zip6 antibody in hopes of detecting a protein of the expected molecular mass. Exhaustive attempts were made to do so but we were unsuccessful (data not shown). We discussed this discrepancy with the manufacturer who was unable to offer a reasonable solution or helpful suggestion other than the explanation that “this sometimes happens”. While the antibody was clearly immunoreactive against the peptide, these data indicated that our newly produced antibody could not be used for our proposed studies due to inability of the antibody to detect endogenous Zip6 at the expected molecular weight and that reported by other investigators. As we were not able to determine what might have led to this problem, we were unwillingly to commit to the production of a second Zip6 antibody. In addition, by the time we had received our antiserum, we had begun essential studies which required the transfection of tumorigenic T47D cells. Transfection of T47D cells turned out to be extremely difficult and required greater financial investment than expected (see Task 2). Therefore, experiments in the proposal were reprioritized and carefully planned to minimize the amount of antibody required. Dr. Huang was willing to share the last of her Zip6 antibody allowing us to complete these studies and we are indebted to her generosity.

In summary, results outlined in Task 1 of our proposal clearly identified several other Zn transporters as targets for future study. In particular, ZnT2 is an interesting candidate as it is responsible for Zn accumulation into vesicles. Thus if dysregulated, ZnT2 over- or under-expression may result in hyper-accumulation of Zn or hyper-sensitivity to excess

cytoplasmic Zn, respectively. Secondly, we determined that while Zip6 mRNA level is significantly lower in tumorigenic T47D cells, Zip6 protein level is significantly higher and may be mis-localized relative to normal breast cells. It is interesting to note that studies from breast cancer patients have observed an inverse relationship between Zip6 mRNA and protein abundance and between low Zip6 expression and higher grade tumors and poor prognosis. Thirdly, we determined that HC11 cells were not an appropriate model of studying Zip6 regulation and function as mRNA expression is very low and Zip6 protein is not translated. It should be noted that we treated HC11 cells with prolactin and estrogen in an attempt to increase Zip6 protein abundance but these attempts were not successful. Finally, while attempts thus far have been unsuccessful at identifying the specific intracellular compartment, studies outlined in Task 2 aimed to determine if cellular function was affected by the over-expression of Zip6 protein and most importantly, if these effects could be rescued by genetically "normalizing" Zip6 expression in tumorigenic T47D cells.

Task 2. To determine if Zip6 plays a role in apoptogenic mechanisms

A. Generation of Zip6-attenuated tumorigenic T47D cells

As we determined that Zip6 was over-expressed in T47D cells, our first objective was to attenuate Zip6 expression in T47D cells with the aim of determining if over-expression of Zip6 was associated with impaired apoptogenic mechanisms. We have successfully used Lipofectamine 2000 (a standard transfection reagent utilizing a liposomal transfection method) to transfect numerous cell lines to generate over-expressing and attenuated derivatives. As illustrated in Figure 10, tumorigenic T47D cells were transiently transfected with two different Zip6-specific siRNAs using Lipofecatamine 2000. Unfortunately, attempts were unsuccessful at optimizing experimental conditions allowing for the attenuation of Zip6 expression in tumorigenic T47D cells, which are a notoriously difficult cell line to transfect. We therefore explored the potential of using the Amaxa Nucleofector System which has been utilized to transfect difficult-to-transfect cell lines such as T47D cells. This transfection system is based on electroporation with defined electrical parameters for specific cell types, has a high transfection efficiency and has been reported to attenuate gene expression in a few hours. We were fortunate in that a colleague in our department was willing to share this piece of equipment with us, with the understanding that we would purchase our own transfection reagents. This was a large expense we did not anticipate. Importantly, using the Amaxa Nucleofector System, we were able to significantly attenuate Zip6 mRNA expression compared with mock-transfected cells (Figure 11A) which was critical to our completion of the proposal. Importantly, the reduction in Zip6 mRNA level resulted in a significant reduction in Zip6 protein abundance compared with the mock-transfected cells (Figure 11B). Based on the efficient mRNA and protein suppression of Zip6 in tumorigenic T47D cells, we chose to utilize the Amaxa Nucleofector System in our subsequent experiments to elucidate potential physiological consequences of Zip6 over-expression in tumorigenic T47D cells.

<u>Documentation that Zip6 attenuation affects cellular Zn pools</u>

Once we were able to successfully attenuate Zip6 expression, our first objective was to confirm that Zip6 attenuation significantly affected cellular Zn levels. As Zip6 is a Zn importer, we first aimed to measure Zn uptake using ^{65}Zn in Zip6-attenuated cells. Unfortunately, these experiments yielded inconsistent results. We speculate that this inconsistency was most likely due to a number of factors; A) the limited amount of Zip6 protein which we documented as expressed on the cell surface of tumorigenic T47D cells; and B) the over-expression of several other Zn importers (Zip1, Zip8 and Zip10) and the Zn exporter ZnT1. Together we suspect these

factors may have confounded our results in the following manner: ^{65}Zn can be taken up by the cell and once taken-up it can be exported, thus integration of Zn transporting processes, combined with our identification of the over-expression of several key players in this process (as outlined in Task 1 complicated the interpretation of data collected from the experiments we proposed in Task 2. We next aimed to determine if the Zn transporting function of Zip6 was significantly affected using a novel approach thus validating that Zn import was indeed reduced in Zip6-attentuated cells. To do so, we utilized two different methods. Firstly, FluorZin-3 is a Zn-specific fluorophore that upon binding to Zn, traps the Zn within the cell and fluoresces. Thus the interaction between FluorZin-3 and Zn provides us with a unique non-radioactive method to quantify changes in vesicularized (labile) Zn pools (21-23).We capitalized on this property and developed a fluorometric assay in which we utilized FluorZin-3 as a sensitive intracellular Zn sensor. As illustrated in Figure 12, FluorZin-3 fluorescence was significantly lower in Zip6-attenuated cells compared with mock-transfected cells, suggesting that cellular Zn pools were significantly reduced by Zip6-attenuation. As mentioned previously, we determined that the majority of Zip6 was localized in an intracellular compartment in tumorigenic T47D cells. Of critical interest is determining whether or not the Zip6 protein that is not plasma membrane-associated is actually functional. Due to the fact that Zip proteins orient Zn transport into the cytoplasm, we reasoned that if the Zip6 which resides intracellularly is functional, it may participate in the transport of Zn from an intracellular, vesicular pool into the cytoplasm. Therefore, if we attenuated Zip6 in tumorigenic T47D cells, in which ~90% of Zip6 is located within the cell, the amount of Zn in vesicular pools should actually increase. As mentioned above, this was not our observation. Indeed, Zip6 attenuation decreased FluorZin-3 fluorescence, suggesting that intracellular Zip6 may not function to transport Zn out of an intracellular compartment. While this may suggest that intracellular Zip6 is non-functional, it is just as likely that intracellular Zip6 traffics to the plasma membrane to import Zn from the exoplasmic space in response to an intrinsic or extrinsic cue similar to other Zip proteins (14,24-27). The functionality of intracellular Zip6 remains not understood. To verify that Zip6-attenuation does significantly reduce cellular Zn levels, we next utilized a luciferase reporter assay as a second method of sensing intracellular Zn pools. Cells were co-transfected with a luciferase reporter construct containing a 4X-Metal-response element (4X-MRE). This novel transcription-based Zn biosensor is based on the endogenous capacity of cells to activate metal responsive transcription factor-1 (MTF-1) and bind to metal responsive elements (MRE) in the promoter region of specific genes. Zinc activation of MTF-1 and subsequent binding to the reporter gene results in luminescence. Using this method we are able to verify subtle changes in cytoplasmic Zn levels. As illustrated in Figure 13, cells expressing the luciferase reporter construct that also had reduced expression of Zip6 had significantly lower luminescence compared with mock-transfected cells. Together these data clearly indicate that Zip6-attenuation significantly reduced cytoplasmic Zn levels in tumorigenic T47D cells. We interpret these data to indicate that while the majority of Zip6 is localized intracellularly in tumorigenic T47D cells, it does not appear to import Zn into the cytoplasm from an intracellular, vesicular pool suggesting that it is either A) non-functional; or B) is functional, but resides in an intracellular compartment that cycles to the plasma membrane as has been determined for other Zn importers such as Zip1, Zip3 and Zip4 (24-27).

B. Establishment of a relationship between Zip6 and mitochondrial function

Once we had conclusively determined that expression of Zip6 modulates cellular Zn pools we aimed to explore the functional consequences of its over-expression in T47D cells. One line of reasoning we proposed was that increased Zip6 abundance would increase cellular Zn pools and result in altered mitochondrial function. In keeping with the goals of the Concept Award, we proposed two avenues of exploration with respect to “altered mitochondrial function” and aimed

to 1) determine if cellular energetics were impaired; or 2) determine if apoptogenic mechanisms were affected.

Zip6 and mitochondrial (m-)aconitase activity

Mitochondria function has been hypothesized to play a role in the progression of epithelial malignancy in cells that have high requirements for Zn such as breast and prostate cells. It is hypothesized that a role of Zn in energy production is to limit the rate of citrate oxidation, thereby preventing the transformation of normal cells into citrate-oxidizing, hyper-energetic malignant cells. The production of ATP in mitochondria is dependant on citrate oxidation which is in part positively regulated by mitochondrial (m)-aconitase activity. Others have shown that high cellular Zn concentration inhibits m-aconitase mRNA, protein and subsequent activity in prostate carcinoma cells (28-30). Therefore, we aimed to explore the role of Zn imported through Zip6 on m-aconitase activity with the hypothesis that Zip6-attenuation would result in reduced Zn import and increased m-aconitase activity. Our first objective was to directly determine if mitochondrial Zn pools are reduced in Zip6-attenuated cells, thereby giving us a direct link between Zip6-mediated Zn import and mitochondrial function. To do so, we exploited the properties of another Zn-specific fluorophore that fluoresces upon binding to Zn pools exclusively in mitochondria (RhodZin-3, (23)). Using this fluorophore, we developed a fluorometric assay allowing us to quantify changes in mitochondrial Zn pools. As illustrated in Figure 14, RhodZin-3 fluorescence was significantly lower in Zip6-attenuated cells compared to mock-transfected cells, indicating that although our studies clearly documented that Zip6 does not reside in mitochondria, aberrant expression of Zip6 can indirectly modulate mitochondrial Zn levels and as such may affect mitochondrial function. To test this hypothesis, tumorigenic T47D cells were transiently transfected with Zip6 siRNA for 48 h to attenuate Zip 6 expression, mitochondria were isolated and then assayed for m-aconitase activity. As shown in Table 1, we did not observe a robust or consistent affect on m-aconitase activity in Zip6-attenuated (KO) cells. We speculate our inability to detect a significant effect reflected the limited amount of mitochondria we were able to isolate as a consequence of the parameters required for optimized transfection with the Amaxa Nucleofactor System. **With that said, our data preliminarily suggests that m-aconitase activity may be lower in Zip6-attenuated cells and we are continuing to follow this line of reasoning with the aim of implicating aberrant mitochondrial Zn levels with decreased ATP production which is beyond the scope of this proposal.**

Zip6 and cytoplasmic cytochrome c oxidase release

Our second avenue of exploration proposed that Zn imported through Zip6 regulates apoptogenic mechanisms. Apoptosis is characterized by distinct morphological and biochemical changes which are orchestrated through activation of either mitochondrial or receptor mediated events. The intrinsic (or mitochondrial) pathway of apoptosis is triggered following damage to the mitochondria activated by intra-cellular events, which increases the permeability of the inner mitochondrial membrane, and subsequently results in mitochondrial matrix swelling followed by release of apoptogenic proteins such as cytochrome c. The release of cytochrome c into the cytosol initiates activation of caspases which then triggers DNA fragmentation as the final step in the apoptotic cascade. It has been appreciated for a long time that alterations in cellular Zn levels result in apoptosis (31).

As our results indicated that Zip6 indirectly modulates mitochondrial Zn pools, our next objective was to explore the potential role of Zip6-mediated Zn import on mitochondria-mediated apoptosis. In doing so, we first determined whether a reduction in Zip6 protein would initiate mitochondrial release of cytochrome c, the initial effector of the apoptotic cascade and

result ultimately in apoptosis. Valinomycin was used as a positive control as it has been shown to induce apoptosis by inducing mitochondria permeability. Intriguingly, our results indicated that Zip6 gene suppression resulted in a significant reduction in the amount of cytochrome c released from the mitochondria compared to mock-transfected cells (Figure 15). As apoptosis is inhibited in cancer cells, we had postulated that reduced mitochondrial Zn levels resulting from Zip6 attenuation would serve to "normalize" apoptogenic mechanisms, thus increasing cytochrome c release from mitochondria and stimulating apoptosis.

Zip6 and mitochondrial membrane potential

Based on this unexpected data we then turned our attention towards upstream pre-apoptogenic events, exploring if the reduction in cytochrome c release resulted directly from alterations in A) mitochondrial membrane permeability which is regulated by B) Bcl-2 family members, such as Bax. To link the Zn-transporting activity of Zip6 with mitochondria membrane permeability and ultimately apoptosis, we examined effects of Zip6 attenuation on alterations in mitochondria membrane potential using the fluorescent dye, JC-1. In cells with intact mitochondria, JC-1 aggregates in mitochondria and emits red fluorescence. In contrast, when mitochondrial membrane potential is compromised, such as that which occurs during apoptotic mitochondrial depolarization, JC-1 dye does not form aggregates and instead emits green fluorescence. Thus alterations in mitochondrial membrane potential can be assessed by changes in the ratio of red:green fluorescence and by nature of this bioassay, pre-apoptotic cells would have greater mitochondrial membrane permeability and a lower ratio of red:green fluorescence. To determine effects of reduced Zip6 expression on mitochondrial membrane potential, tumorigenic T47D cells were transfected with Zip6 siRNA and treated with JC-1. Zinc (75 μM) was utilized as a positive control and cells treated with Zn resulted in a significant reduction in membrane potential compared to non-treated cells, confirming that Zn accumulation causes depolarization in tumorigenic T47D cells (Figure 16). Thus far we have not been successful in quantifying changes in mitochondrial membrane potential in mitochondria isolated from Zip6-attenuated cells (Figure 16). These results can be interpreted in one of three ways; either Zip6 attenuation does not result in decreased mitochondrial membrane potential, further optimization of our method is required, or JC-1 is not a sensitive enough marker of subtle alterations in mitochondrial membrane potential. With that said, based on our data which indicates that Zn concentration and cytochrome c release from mitochondria is indeed lower in Zip6-attenuated cells, it is reasonable to assume that mitochondrial membrane permeability is likely lower in response to Zip6 attenuation and continued optimization of our assay is necessary.

Therefore, we proceeded to develop a more sensitive indicator of altered mitochondrial membrane permeability and aimed to determine if Zip6 attenuation directly results in increased pores in the mitochondrial membrane (an upstream event leading to increased permeability). Mitochondrial membrane permeability is regulated by the translocation and subsequent oligomerization of Bax (homo- and heterocomplexes), resulting in the formation of mitochondrial membrane pores, leading to changes in mitochondria potential (32,33) and subsequently resulting in the release of cytochrome c. Previous studies have reported that Zn induces mitochondria mediated apoptosis via Bax translocation to mitochondria suggesting increased abundance of pores in malignant prostate cells (15,16). Thus we hypothesized that decreased cellular Zn levels resulting from Zip6 attenuation would reduce Bax oligomerization, thereby decreasing mitochondria membrane permeability and resulting in decreased cytochrome c release into the cytoplasm. To develop this technique, Zn treatment (75 μM) was used as a positive control. Extracts of T47D cells were lysed in buffer containing different amounts of digitonin and Bax oligomers were cross-linked as previously described (34), then Bax oligomerization was assessed by immunoblotting. Our results indicated that in non-treated T47D cells Bax exists in both its monomeric (~23 kDa) and oligomeric (~260 kDa) forms (35),

implicating constitutive Bax activation (and possibly increased mitochondrial membrane permeability) with our observation of endogenous sub-lethal cytochrome c release in tumorigenic T47D cells. The use of Zn as a positive control to induce mitochondria-mediated apoptosis resulted in increased Bax oligomerization (Figure 17). We interpret these results to indicate that our assay is adequate to determine if alterations in cellular Zn pools induces Bax oligomerization in T47D cells. We are currently in the process of exploring effects of Zip6 attenuation on Bax oligomerization.

Zip6 and caspase activation

Our next objective was to explore the downstream consequences of Zip6 over-expression in tumorigenic T47D cells. We first aimed to determine if the reduction in cytochrome c release as a consequence of Zip6 attenuation subsequently resulted in reduced caspase activity which would implicate Zip6 in the regulation of apoptogenic mechanisms. In keeping with our proposal we initially undertook a candidate approach and began with determining effects of Zip6 attenuation on caspase activity and we proposed to use immunoblotting to explore this line of reasoning. We began with the most upstream effector, caspase-9. Following the release of cytochrome c from the mitochondria, procaspase-9 (~47 kDa) is subsequently cleaved (~38 and 17 kDa) and is thus activated. Based on our data which indicated that cytochrome c release was reduced by attenuating Zip6 expression, we postulated that constitutive caspase-9 cleavage would also be reduced. To first optimize our experimental conditions we treated T47D cells with valinomycin for 24 h, collected the total cell lystate and immunoblotted for caspase-9. As shown in Figure 18, while we were able to detect procaspase-9, we were unable to detect cleaved caspase-9 fragments (~38 and 17 kDa) using valinomycin as a positive control. In fact, we were unsuccessful in detecting caspase-9 cleavage by immunoblotting using a variety of experimental conditions. Instead of continuing with a candidate approach which was expensive and time consuming, we aimed to utilize a caspase activity screen using a fluorometric detection system that would allow us greater sensitivity and flexibility. This assay afforded us A) the ability to measure changes caspase activity and not pro-caspase cleavage; and B) the ability to screen for changes in four different caspases at once. This was an important aspect of our proposal as our optimized transfection method is expensive and thus cost efficiency was of critical importance. Our data clearly indicated that Zip6 attenuation significantly reduced caspase activity overall (Table 2), indicating that apoptogenesis is further impaired when Zn import through Zip6 is reduced.

Zip6 and DNA fragmentation

The final stage of apoptosis is DNA fragmentation which is a hallmark of apoptosis that results from caspase activation. DNA fragmentation is the result of internucleosomal DNA cleavage producing 180-200 base pair fragments which are visible by ethidium bromide staining of isolated DNA electrophoresed through agarose. To further support our developing interpretation that over-expression of Zip6 in breast cancer cells is not anti-apoptotic, we aimed to visualize changes in apoptogenesis using a DNA fragmentation assay. To first optimize our assay, T47D cells were incubated with Zn (75μM, as a positive control) to induce apoptosis and DNA laddering was evaluated by electrophoresis. As illustrated in Figure 19, while our positive control of Zn treatment resulted in a minimal amount of DNA laddering, no basal DNA laddering was detected in T47D cells. Thus, without being able to visualize a basal level of DNA laddering, a "reduction" in DNA laddering which we would interpret to reflect our observation of reduced cytochrome c release and caspase activity would be impossible to detect. Therefore, this line of reasoning was abandoned. The fact that these cells display "sub-lethal" release of cytochrome c, endogenous activation of caspase activity and yet no apparent DNA laddering is (apoptosis), in itself an interesting observation. **Taken together, our data provides evidence**

that Zn imported via Zip6 modulates mitochondrial Zn level and affects cytochrome c release ultimately caspase activity, but counter intuitively our data suggests that Zip6 over-expression which has been observed in breast cancer biopsies and now in tumorigenic T47D cells does not functionally suppress apoptogenic mechanisms and thus may not be an initial event in cancer transformation. In fact "normalizing" Zip6 expression appears to further compromise apoptogenesis in tumorigenic T47D cells, suggesting that Zip6 may actually function as a "tumor-suppressor". Studies are ongoing to verify that these events result from decreased mitochondrial membrane permeability due to decreased Bax oligomerization which are beyond the scope of this proposal.

C. Effects of Zip6 attenuation on functional outcomes in T47D cells

An important consideration relates to the downstream functional consequences of Zip6-mediated Zn import. Our emerging data suggests that Zip6 over-expression in tumorigenic T47D cells may not contribute to the cancer phenotype but may in fact act as a "tumor-suppressor". Exploring the functional relevance of Zip6 over-expression may thus be of critical importance in developing novel therapies. We proposed to utilize a PCR-based breast cancer array to explore downstream consequences of Zip6 attenuation. PCR-based breast cancer arrays which focus on either cell signaling molecules or cell adhesion pathways are commercially available. In reviewing carefully the targets of these PCR-based screens we were uncertain as to which screen would provide the most useful information, given the data we had generated from the experiments outlined above from our proposal. Therefore we chose to first conduct some preliminary experiments to guide our choice. We reasoned that if Zn transported through Zip6 plays a role in "tumor suppression", perhaps Zip6 attenuation would increase tumor formation. Intercellular interactions play important roles in the development and progression of cancer. Reductions in intercellular adhesion allow cancer cells to detach at the primary site of origin, resulting in loss of cellular polarity. E-cadherin is an intercellular adhesion molecule, and has been shown to mediate the epithelial cell–cell interactions. Loss of E-cadherin expression has been associated with high histologic tumor grade, advanced clinical stage, and poor prognosis of patients with breast cancer. It has been previously illustrated that Zip6 expression is positively associated with expression of E-cadherin (36). This suggests that Zn imported via Zip6 may modulate cellular adhesion as E-cadherin is a tumor suppressor and is important in the regulation of adhesion and motility (37,38). Thus we hypothesized that reduced cellular Zn level resulting from Zip6 attenuation would decrease E-cadherin expression and increase tumor formation. We therefore first determined effects of Zip6 attenuation on E-cadherin mRNA expression and the ability of tumorigenic T47D cells to form tumor colonies. Zip6 expression was attenuated for 48 h and E-cadherin mRNA level was assessed by Q-PCR. As illustrated in Figure 20, we observed a concomitant and significant reduction in E-cadherin mRNA expression compared to mock-transfected cells. As a functional consequence of reduced E-cadherin expression we next aimed to assess tumorigenicity. To do so we assessed effects of Zip6 attenuation on tumor formation of tumorigenic T47D cells cultured in soft agar. We arbitrarily characterized a "cluster" of >3 cells as a "tumor" and counted the number of "tumors" and the total number of cells in ten different fields (10X magnification). Our preliminary data illustrated that Zip6 attenuation was associated with increased tumor colony formation compared with mock-transfected cells. Interestingly, Zip6 attenuation also resulted in greater cell numbers compared with mock-transfected cells (Table 3). **These preliminary data suggested to us that the cell adhesion pathway PCR-based array may provide an interesting avenue of investigation to search for novel targets resulting from Zip6-mediated Zn import. Unfortunately, due to financial and time constraints we were unable to complete this objective and studies are currently underway to explore this avenue from other funding sources. Taken together, these data further**

support our developing evidence that Zip6 may function as a "tumor-suppressor" in T47D cells.

In summary, the results outlined in Task 2 counter-intuitively suggest that Zip6 over-expression in tumorigenic T47D cells, if functionally relevant, may play a role as a "tumor suppressor" through modulation of apoptogenesis and/or cell adhesion mechanisms. Further studies are required to understand the role of Zip6 in these processes but will certainly provide important information regarding the integration between cellular Zn metabolism and tumorigenesis or metastasis.

Task 3. To determine if prolactin regulates Zip6 differentially in breast cells which express endogenous prolactin receptor (normal, HC11; carcinoma, T47D)

A. Effects of prolactin on Zip6 expression and localization

Several recent studies have found an association between hyperprolactinemia and breast cancer. Although the mechanisms behind these observations are not understood, our previous studies indicate that PRL increases Zn transport in breast cells through increased activity of Zn transporting mechanisms. Moreover, as we and others (3,4) have clearly shown that Zn metabolism is dysregulated in breast cancer cells, we hypothesize that PRL may further dysregulate cellular Zn pools. As a result, our principal hypothesis states that hyperPRL increases cellular Zn uptake through alterations in Zip6 expression and localization and subsequently affects apoptogenic mechanisms. To test this hypothesis, we first examined the effect of PRL on changes in cellular Zn uptake using FluorZin-3 as an indicator of cellular Zn pools. We have previously shown that PRL increases Zn uptake in non-cancerous HC11 cells (14). Tumorigenic T47D cells were treated with PRL and intracellular Zn pools were visualized with FluorZin-3. As illustrated in Figure 21, PRL significantly increased cellular Zn pools (Figure 21D-F) compared to cells not treated with PRL (Figure 21A-C), suggesting that in fact hyperPRL can modulate cellular Zn pools in tumorigenic T47D cells as well as normal breast cells. We next investigated whether the increase in cellular Zn level was mediated by increased Zip6 expression. As previously noted, we detected minimal Zip6 mRNA abundance and no Zip6 protein in HC11 cells. Preliminary studies indicated that we were unable to induce Zip6 expression with PRL treatment in HC11 cells. Thus we chose to continue our proposed experiments in tumorigenic T47D cells. To determine if PRL regulates Zip6 expression in T47D cells, we first measured mRNA expression using Q-PCR in T47D cells treated with PRL. Our results indicated that PRL significantly reduced Zip6 expression (<50%) compared to non-treated cells (Figure 22). We next determined if decreased expression of Zip6 mRNA resulted in a subsequent decrease in abundance of Zip6 protein. Interestingly, our data demonstrated that there was no robust affect of PRL on Zip6 protein abundance in T47D cells compared with untreated cells (Figure 23). Finally, we reasoned that PRL may post-translationally regulate the sub-cellular localization of Zip6. Thus, we next used confocal microscopy to determine if PRL treatment potentiates the trafficking of Zip6 to the plasma membrane in T47D cells. As indicated in Figure 24, we determined that PRL did not result in the re-localization of endogenous Zip6 from the intracellular location within which it resides. **Taken together, these data suggest that PRL does not play a major role in Zip6 protein abundance or re-localization in tumorigenic T47D cells, indicating that the PRL-stimulated Zn uptake we detected in T47D cells is not mediated by alteration in Zip6.**

In summary, the results outlined in Task 3 eliminated our line of reasoning that PRL potentiates Zn uptake in tumorigenic T47D cells through alterations in the expression of localization of Zip6. With that said, PRL treatment increased cellular Zn pools which

suggests that hyperprolactinemia may further potentiate the dysregulation of cellular Zn metabolism observed in breast cancer. Further studies are currently underway to explore the cellular consequences of hyperprolactinemia in breast cancer cells, independent of effects on Zip6.

METHODS:

Cell culture - Human tumorgenic (T47D) and normal human mammary epithelial (HME) cells were obtained from the American Type Culture Collection (ATCC). T47D cells were routinely cultured in plastic 75 cm^2 flasks, maintained in "growth medium" containing, RPMI 1640 (SIGMA, St. Louis, MA) supplemented with fetal bovine serum (10%), insulin (0.2 units/mL), sodium pyruvate (1.0 mM) and penicillin/streptomycin (1%). HME cells were cultured in 75 cm^2 flasks and grown in Medium 171 (Invitrogen, Carlsbad, CA) supplemented with mammary epithelial growth supplement (Invitrogen). HC11 cells were a gift from Dr. Jeffery Rosen (Houston, Texas) and used with permission of Dr. Bernd Groner (Institute for Biomedical Research, Frankfurt, Germany). Cells were routinely maintained in a proliferative phenotype by culturing in "growth medium" (RPMI 1640 supplemented with 10% fetal bovine serum, insulin (5 µg/mL), EGF (10 ng/mL; Sigma) and gentamycin 50 mg/L; Sigma). Cells were maintained in 5% CO_2 at 37 °C humidified atmosphere.

Zip6 mRNA isolation and real-time quantitative RT-PCR - Total RNA was isolated using TriZOL (Invitrogen, per manufacturer's instruction) and diluted to 1 µg/µL in RNase-free water as previously described (20). cDNA was generated from 1 µg RNA by reverse transcription (Applied Biosystems, Foster City, CA) performed at 48 °C for 30 min followed by 95 °C for 5 min. Real-time PCR was performed using the cDNA reaction mixture (1.0 µL) using the DNA Engine Opticon 2 System real-time thermocycler (BioRad, Hercules, CA) coupled with SYBR Green technology (BioRad) using species and gene-specific primers Primers were designed by Primer 3 Input v4.0. The PCR cycling parameters were as follows: 50 °C, 2 min; 95 °C, 10 min; 40 cycles of 95 °C, 15 s; 60 °C, 1 min; followed by 95 °C, 15 s. (See Tables 4 and 5).

Production, purification and verification of antibody purification - A peptide fragment of Zip6 (VSEPRKSFMYSRNTNDN) was synthesized (Genemed Synthesis, TX) with an additional cysteine residue for conjugation to keyhole limpet hemocyanin at the C-terminal end. For purification, Zip6 peptide (2 mg) was conjugated to an affinity-purification column (Sulfolink purification kit; Pierce Biotechnology) and antibody was purified from rabbit antiserum according to the manufacturer's instructions. To demonstrate antibody specificity, affinity-purified Zip6 antibody (1 mg/ml) was pre-incubated with Zip6 peptide (1 mg) in 5% (w/v) non-fat milk in PBS-T (PBS, 0.1% Tween) for 2 h at room temperature (25°C) prior to immunoblotting of cell proteins which had been separated by electrophoresis and transferred to nitrocellulose (see below), as previously described (39).

Cellular Zip6 protein levels and immunoblotting- Cells were washed in PBS, scraped into lysis buffer containing protease inhibitors as previously described (REF) and sonicated for 20 s on ice. Cellular debris and nuclei were pelleted by centrifugation at 500 x g for 5 min and protein concentration of the post-nuclear supernatant was determined by Bradford. To isolate crude membrane fraction, the post-nuclear supernatant was centrifuged at 100,000 x g for 20 min at 4ºC. Protein (50-100 µg) was diluted in Lammelli sample buffer containing DTT (100 mM) and incubated at 95ºC for 5 min. Proteins were separated by electrophoresis, transferred to nitrocellulose for 60 min at 100 V then immunoblotted with affinity-purified rabbit anti-Zip6 antibody (1:1000, a gift from Dr. Liping Huang, Western Human Nutrition Research Center, Davis, CA), anti-bax (1:1000; Cell Signaling, Danvers, MA) anti-cytochrome C (0.5 µg/mL; BD

Biosciences, San Jose, CA), cleaved caspase-9 (1:1000; Calbiochem, Gibbstown, NJ), calreticulin (1:1000; Abcam, Cambridge, MA), or mouse β-actin and detected with horseradish peroxidase-conjugated IgG. Proteins were visualized by chemiluminescence (Femto; Thermo-Fisher) after exposure to autoradiography film and relative band density and molecular mass relative to standard molecular mass markers (Amersham Pharmacia) was assessed using the Chemi-doc Gel Quantification System (Biorad).

Cell surface biotinylation - Sulfo-NHSS biotin (Pierce) was used to label cell surface proteins to detect endogenous Zip6 at the plasma membrane, as previous described (39)with slight modifications. Cells were cultured until confluent and biotinylated with Sulfo-NHSS biotin (0.5 mg/mL) at room temperature for 30 min. Cells were washed twice with 50 mM Tris, pH 8.0 followed by three washes with ice-cold PBS, scraped into cold lysis buffer (50 mM Tris pH 7.4, 2 mM EDTA, 2 mM EGTA, plus protease inhibitors) and sonicated for 30s on ice. The crude membrane fraction was pelleted by ultracentrifugation at 100,000 x g for 30 min and resuspended in lysis buffer containing NaCl (0.1 M) and membranes were solubilized with SDS (final concentration to 0.2%) at 60ºC for 5 min and Triton X-100 (final concentration to 1%) then briefly sonicated on ice. Insoluble material was pelleted by ultracentrifugation at 100,000 x g for 20 min and supernatant was incubated with 75 uL of a 1:1 slurry of Ultralink-neutravidin beads (Pierce) while rocking at room temperature for 1 h. Biotinylated plasma membrane proteins affinity-precipitated on avidinated beads and pelleted by centrifugation at 5,000 rpm for 1 min and washed four times with PBS + 1% Triton X-100. The non-biotinylated intracellular membrane proteins (supernate) were collected by centrifugation at 100,000 x g for 20 min and resuspended in Lammelli buffer containing DTT (100 mM). Biotinylated proteins were eluted from the avidinated beads by heating to 95ºC in Lammelli buffer containing DTT. Samples were separated by electrophoresis and immunoblotted using Zip6 antibody, as described above.

Immunofluorescence - To determine the sub-cellular localization of endogenous Zip6 cells were plated onto glass coverslips and fixed in phosphate buffered-paraformaldehyde (4%), pH 7.4 for 10 min, washed in PBS, and either permeabilized with Triton X-100 (0.2% in PBS) for 10 min or left non-permeabilized. Cells were incubation with Zip6 antibody. After extensive washing with PBS, Zip6 antibody was detected with Alexa 488-conjugated anti-rabbit IgG (1 µg/mL, Invitrogen) for 45 min at room temperature shielded from light. Cells were washed, mounted and coverslips sealed. Sub-cellular co-localization markers were as follows: nucleus TOPRO-3 (1:1000; Invitrogen), endoplasmic reticulum (mouse, anti-human calnexin, 2.5 µg/mL; Abcam); and Cox VI (mouse, anti-human cytochrome c-oxidase subunit IV; 2.5 µg/mL ; Invitrogen). Co-localization antibodies were detected with Alexa 568-conjugated anti-mouse or anti-goat IgG (Invitrogen).Immunofluorescent imaging was performed using an Olympus FV1000 (Inverted Olympus IX-81**)** Laser Scanning Confocal Microscope (Olympus America Inc., Melville, NY) with UPlanApo 60X oil lens N.A. 1.42 and digital images were captured sequentially (FV10-ASW version 1.6).

Differential centrifugation – For sub-cellular fractionation, cells were washed in PBS, scraped into lysis buffer containing protease inhibitors as previously described (14)and homogenized with glass dounce homogenizer with a tight pestle for 30 strokes. The nuclear fraction (fraction 1) was pelleted by centrifugation at 500 x g for 10 min at 4ºC. The post-nuclear supernatant was differentially centrifuged to separate the sub-cellular compartments. To obtain a pellet enriched in mitochondria, the supernatant was centrifuged at 5,000 x g for 10 min (fraction 2). Subsequent supernatants were centrifuged at 15,000 x g for 5 min (fraction 3, enriched in endoplasmic reticulum, endosomes and lysosomes); 100,000 x g for 1 h (enriched in plasma

membrane, Golgi and microsomes); 150,000 x g for 1 h (fraction 4, enriched in cytoplasmic proteins; (fraction 5). Protein concentration of supernatants was determined by Bradford.

Mitochondria isolation – To verify mitochondrial localization of Zip6, cells were scraped into ice-cold MB buffer (10 mM Hepes, pH 7.5, 210 mM mannitol, 70 mM sucrose, 1 mM EDTA) then dounce homogenized using a glass homogenizer. The cell extract was centrifuged at 2,000 x g for 5 min at 4ºC and crude mitochondrial fraction was pelleted by centrifugation at 12,000 x g for 12 min at 4ºC. The crude mitochondria fraction was resuspended in MB buffer and gently homogenized on ice then purified on a discontinuous Nycodenz gradient (22.5% and 9.5% diluted into MB buffer) following centrifugation at 141,000 x g for 1 h at 4ºC. Purified mitochondria were washed twice in MB buffer following centrifugation at 12,000 x g for 12 min. To generate mitochondria devoid of the outer mitochondrial membrane (mitoplasts), purified mitochondria were hypotonically lysed in water on ice for 20 min and pelleted by centrifugation at 15,000 x g for 15 min. To eliminate contaminating sub-cellular membranes, intact mitochondria or mitoplasts (10 μg) were digested with an equal amount of proteinase K (10 μg) on ice for 20 min as indicated. Enzymatic activity was inactivated with PMSF (20 mM) for 20 min on ice and mitochondria were pelleted by centrifugation.

siRNA-mediated gene attenuation - T47D cells were transfected using Amaxa nucleofactor solution (Gaithersburg, MD) following manufacture's instructions. Cells (5 X 10^6/ 0.100 mL) were transfected without or with 200 pmol of SLC30A6-specific (sense: 5'-GGGUUCAGAAAAUUACUUC-3', antisense: 5'-GAAGUAAUUUUCUGAACCC-3') siRNA (Ambion, Applied Biosystems, Austin, TX) in medium containing FBS and antibiotic-free medium for 48-72 h.

Mitochondria aconitase assay – Cells were prepared as previously described with slight modifications (40). Briefly, cells were rinsed with PBS, lysized buffer containing sucrose (0.25 M), Hepes (50 M) and digitonin (0.007%) and incubated on ice for 5 min. Samples were centrifuged at 1800 g for 8 min at 4°C and pellets were resuspended in lysis buffer and re-centrifuged. Pellets were resuspended in buffer containing Tris-HCl, pH 7.4 (50 mM), Trition X-100 (0.2%), DTT (1 mM) and 1X proteinase inhibitors. Supernate was collected after samples were vortexed, incubated on ice and centrifuge at 8000 g for 5 min at 4°C. M-aconitase activity was measure in solution containing Tris-HCl (100mM), MgCl2, pH 8.0 (1 mM), NADP (1mM), Sodium Citrate (1 mM) and isocitrate dehydrogenase (1 U/rxn) at 340nm at 37°C in 96-well plates.

Cytochrome c release – T47D cells were transfected with Zip6 siRNA as previous described above or treated with valinomycin (10 μM; SIGMA) overnight. Cells were collected in buffer containing sucrose (250 mM), hepes (20 mM), and EDTA (1mM) with freshly added 1X protease inhibitors. Cells were homogenized with glass dounce homogenizer (15-20 strokes) and centrifuge at 15,000 g for 15 min at 4°C. Pellet (crude mitochondria) was re-suspended in buffer and supernate was centrifuge at 20,000 g for 15 min to remove any remaining non-soluble components as previously described (41). Samples were prepared for immunoblotting for cytochrome c as described above.

Caspase activity – To determine the effect of Zip6 gene attenuation on caspase activity, cells were transfected as described above and cultured for 48 h. Samples were collected for 96-well plate SensoLyte Fluorimetric Caspase Profiling Kit as recommended by the manufacture. Media was removed, cells were scraped in 1X lysis buffer and incubated at 4°C for 30 min. Cell suspension was centrifuged at 2500 g for 10 min at 4°C and samples (50 μL) were added to

substrate containing wells to initiate enzyme reaction. Fluorescence was measured at Ex 405/ Em 520 nm continuously and data recorded over time for 60 min. Protein concentration of supernatants was determined by Bradford.

DNA fragmentation – T47D cells were cultured in 6-well dishes for 3-4 days and then treated without or with $ZnSO_4$ (75 μM) overnight. Samples were prepared as previously described (42) with modifications. Cells were lyzed with hypotonic lysis buffer containing Tris-HCl, pH 8.0 (10 mM), EDTA (10 mM) and SDS (1.0%). Cells were incubated with RNases (0.1 mg/ml; SIGMA) for 1 h at 37°C. To digest proteins cells were incubated with proteinase K (1 mg/mL; Promega) for 2 h at 50°C. DNA was extracted 3X with phenol, chloroform, and isoamyl alcohol mixture (25:24:1; SIGMA) following the manufactures instructions. Equal volumes of phenol:chloroform:isoamyl alcohol solution were added to samples, mixed and centrifuge at 12,000 g for 5 min at room temperature. The aqueous phase was separated and DNA was precipitated with equal volumes of isopropyl alcohol and stored overnight at -20 °C. DNA was rinsed with 70% ethanol and centrifuged at 12,000 g for 10 min at 4 °C. Pellet was resuspend in TE buffer and DNA concentration at 260 nm was determined. Equal amounts of DNA were loaded and electrophoretically (60V) separated on a 1.5% agarose gel containing 1 μg/ml ethidium bromide. Band were visualize under UV to determine ideal separation.

Mitochondrial membrane potential - To determine the effect of Zip6 (LIV-1) gene silencing on mitochondria potential, cells were transfected with Zip6 (LIV-1) specific siRNA as described above. Cells were plated onto 96-well plates for 48h and the mitochondrial potential was analyzed by JC-1 (Invitrogen). Briefly, cells were rinsed with 1X PBS, pH 7.4 and incubated with JC-1 dye (2 μM) dye for 30 min at 37°C. Cells were rinsed with 1X PBS, pH 7.4 and fluorescence intensity was measured. Red (ex. 560 nm–em. 590 nm) and green fluorescence (ex. 485 nm–em. 520 nm) was measured at 25°C using FLUOstar OPTIMA plate reader (BMG Labtech) spectrofluorimeter. Cellular protein concentration was determined by Bradford assay and fluorescence measurements were normalized to total protein concentration.

Plasmid generation, transient transfections and luciferase reporter assay - The 4X-MRE (metal-responsive element) pGL3-luciferase reporter was kindly provided Dr. Colin Ducket (Univ. Michigan Medical School, Ann Arbor, MI). Large scale plasmid purification was carried out using the Plasmid Midi Kit (Sigma). For luciferase reporter assay, T47D cells were plated into 24-well plates and transfected using Amaxa nucleofactor kit, as mentioned above. Each well was tranfected with either pGL3 empty vector (0.8 μg) or 4X-MRE-pGL3 luciferase reporter (0.8 μg) and pRL-TK renilla vector (0.05 μg) without or with Zip6 siRNA (200 pmol). After 48 h, cells were treated with $ZnSO_4$ (7 μM) for 24 h to activate the promoter and then analyzed for luciferase activity as previously described (43). After incubation, cells were rinsed with 1X PBS and harvested in 1X passive lysis buffer (Promega, Madison, WI) following manufacture's instructions and measured by luminometry (Turner Biosystems, Sunnyvale CA) using Dual-Luciferase reporter assay system (Promega) for firefly and renilla luciferase activity. Relative light units (RLU) were determined by the ratio of firefly:renilla luciferase activity.

FluorZin-3 and RhodZin-3 fluorometry assay – To verify that Zip6 facilitates the efflux of Zn out of vesicles containing labile Zn, cells were transiently transfected with Zip6 siRNA as described above. Cells were rinsed with 1X PBS, pH 7.4 and loaded with FluorZin-3 AM (1 μM, Invitrogen) as recommended by the manufacturer in Opti-MEM containing 0.2% Pluoronic acid 127. Cells were rinsed two times with PBS, pH 7.4, incubated for 30 min at 25°C with constant shaking then treated with $ZnSO_4$ (10μM) for 30 min at 37°C. Fluorescence of FluorZin-3 (em. 495nm–ex. 516nm) was measured at 25°C using FLUOstar OPTIMA plate reader (BMG

Labtech) spectrofluorimeter with FLUOstar OPTIMA software version 1.32R2. Cellular protein concentration was determined by Bradford assay and fluorescence measurements were normalized to total protein concentration.

Soft agar colony formation – To verify that Zip6 plays a role in tumor formation, cells were transiently transfected with Zip6 siRNA as described above. The agar base was prepared by melting 1% agar in water and mixed with equal parts of RPMI plus 20% FBS to 40°C and allowed to solidify for 15 min at room temperature. The top agarose was prepared by melting 0.7% agarose in microwave in water and mixed with equal parts of RPMI plus 20% FBS to 40°C, allowed to cool and siRNA transfected cells (5×10^6/ 0.100mL) were added and gently poured onto the culture dish. T47D cells were incubated for 72 h at 37°C. Colonies (<3 cells or more) and individual cells were counted using a Zeiss inverted microscope.

Statistical analysis - Results are presented as mean ± standard deviation from triplicate samples from three independent experiments. Statistical comparisons were performed using Student's *t*-test (Prism Graph Pad, Berkeley, CA) and a significant difference was demonstrated at $p<0.05$.

Key Research Accomplishments

- Characterized the differential expression of seven zinc-specific transporters in a cultured tumorigenic breast cancer cell model relative to expression in non-cancerous cells. **This provides numerous novel avenues of investigation regarding the molecular mechanisms responsible for dysregulated zinc metabolism associated with breast cancer.**

- Characterized the aberrant expression of Zip6 and a negative correlation between Zip6 mRNA expression and protein abundance in a cultured tumorigenic breast cancer cell model (T47D) which is similar to that observed in breast cancer tissue biopsies. **This validates T47D cells as an appropriate model of a tumorigenic ductal carcinoma with respect to Zip6 dysregulation and its functional relevance.**

- Determined that while over-expressed, the majority (~90%) of Zip6 protein is located in to an intracellular compartment. This localization is different from that observed in non-cancerous cells (which is associated with the plasma membrane), **indicating that intracellular Zip6 is either A) mis-localized in T47D cells and thus may result in a non-functional protein or suggests that B) Zip6 traffics to the plasma membrane in response to yet unknown intrinsic or extrinsic cues and thus may exacerbate zinc import in response to these cues.**

- Determined that Zip6 regulates cytosolic, vesicular and mitochondrial zinc levels. Attenuation of Zip6 expression reduced cellular zinc pools, reduced sub-lethal release of cytochrome c oxidase from mitochondria and subsequently reduced caspase activation. **This suggests that zinc imported through Zip6 regulates apoptogenic mechanisms but does so in a counter-intuitive manner.**

- Determined that zinc imported through Zip6 regulates E-cadherin expression and thus either directly or indirectly affects cell proliferation and tumorigenesis. Attenuation of Zip6 reduces E-cadherin expression resulting in increased cell proliferation and tumorigenesis. These data suggest that over-expression of Zip6 in tumorigenic breast cells may actually function in as a “tumor-suppressor”. **Critically, zinc import through Zip6 may play a role in metastatic transformation of tumorigenic T47D cells and may provide important insight as to why greater expression of Zip6 protein is associated with lower grade tumors and better prognosis.**

- Determined that while prolactin increased zinc import into tumorigenic T47D cells, these effects are not a consequence of alterations in Zip6 expression or localization. **Nonetheless, this importantly suggests that dysregulation of cellular zinc metabolism in breast carcinomas may be potentiated through zinc transporting mechanisms that remain to be elucidated.**

Reportable Outcomes

1) Abstracts
   a) Era of Hope 2008 – "Dysregulation of Zip6 (LIV-1) is not potentiated by prolactin in tumorigenic breast cancer cells"
   b) American Society of Cell Biology 2008- "Over-expression of Zip6 (LIV1) in tumorigenic breast cancer cells (T47D) cells modulates sub-lethal cytochrome c release and apopotgenesis"

2) Presentations
   a) Era of Hope 2008 (Poster-Shannon L Kelleher, presenter)
   b) American Society of Cell Biology 2008 (Poster-Veronica Lopez, presenter)

3) Funding applied for based on work supported by this award
   a) Summer Research Grant to Farnaz Foolad to pursue the role of ZnT2 in tumorigenic breast cancer cells.
   b) Planned submission of a new Breast Cancer Research Program Concept Award to pursue ZnT2 as a potential target for therapeutic intervention in tumorigenic breast cancer cells.
   c) Planned submission of a new Breast Cancer Research Program Concept Award to explore the role of Zip6 in metastatic transformation.

Conclusion

In summary, results from this study have provided important insight with respect to the functional relevance of Zip6 (LIV-1) dysregulation in tumorigenic breast cancer cells. Through genetic manipulation of Zip6 expression in a cultured tumorigenic breast cancer cell model we have documented that Zip6 functionally provides zinc to cytoplasmic, vesicular and mitochondrial pools. Zip6 over-expression maintains sub-lethal release of cytochrome c and constitutive caspase activity resulting in dampened cell proliferation and tumor formation. We speculated that attenuation of Zip6 expression would result in increased apoptosis; however, preliminary results suggest that decreased zinc import as a result of Zip6 attenuation result in increased cell proliferation and enhanced tumorigenesis. This provides two critical pieces of information; 1) provides important insight regarding mechanisms responsible for the association that has been observed between elevated Zip6 protein abundance and lower histologic grade tumors and better prognosis; and 2) suggests that attenuating Zip6 over-expression as a therapeutic target may result in metastatic transformation. These studies clearly illustrate the importance of understanding the functional relevance of putative prognostic indices prior to pursuing therapeutic intervention. Further studies are clearly needed to verify a role for Zip6 in epithelial-to-mesenchymal transition to assist in understanding the relationship between Zip6 expression, tumor characteristics and metastasis as it relates to relapse free survival.

Secondly, several studies have associated hyperprolactinemia is associated with breast cancer. The significance of this relationship lies in the fact that drugs which induce hyperprolactinemia secondarily to the principal mode of action (e.g. dopamine antagonists such as cabergoline, risperidone and olanzapine) are widely prescribed for the treatment of a range of illnesses including Parkinson's Disease, depression, schizophrenia, behavior disorders, aggression and self-injury in children, adolescents, and adults with mental retardation, pervasive developmental disorders, mood disorders and autism. In many cases, these drugs are prescribed for patients as young as 3 years of age and are chronically administered, thus potentially increasing the risk for the development of breast cancer in an enormous number of individuals.
Our data clearly illustrates that prolactin stimulation does increase Zn uptake into tumorigenic breast cancer cells which are already hyper-sensitized to Zn toxicity suggesting that hyperprolactinemia could further potentiate adverse effects of dysregulated cellular Zn metabolism in breast cancer. Our results indicate that alterations in Zip6 expression or localization can be excluded from the etiology of this relationship. This implicates alterations in the expression or localization of other Zn transporters in the relationship between hyperprolactinemia and dysregulated cellular Zn metabolism in breast cancer. Thus pursuit of these novel targets is of great therapeutic interest. Further studies are critically needed to understand potential adverse consequences of hyperprolactinemia in breast cancer cells as diminished prolactin signaling reduces cell proliferation, delays tumor formation and understanding this relationship may ultimately lead to novel therapies.

References

1. Levenson, C. W., and Somers, R. C. (2008) *Nutr Rev* **66**(3), 163-166
2. Lee, R., Woo, W., Wu, B., Kummer, A., Duminy, H., and Xu, Z. (2003) *Exp Biol Med (Maywood)* **228**(6), 689-696
3. Margalioth, E. J., Schenker, J. G., and Chevion, M. (1983) *Cancer* **52**(5), 868-872
4. Santoliquido, P. M., Southwick, H. W., and Olwin, J. H. (1976) *Surg Gynecol Obstet* **142**(1), 65-70
5. Eide, D. J. (2006) *Biochim Biophys Acta* **1763**(7), 711-722
6. Hashemi, M., Ghavami, S., Eshraghi, M., Booy, E. P., and Los, M. (2007) *Eur J Pharmacol* **557**(1), 9-19
7. Jin, R., Bay, B. H., Chow, V. T., and Tan, P. H. (2001) *Breast Cancer Res Treat* **66**(3), 265-272
8. Kagara, N., Tanaka, N., Noguchi, S., and Hirano, T. (2007) *Cancer Sci* **98**(5), 692-697
9. Tai, S. K., Tan, O. J., Chow, V. T., Jin, R., Jones, J. L., Tan, P. H., Jayasurya, A., and Bay, B. H. (2003) *Am J Pathol* **163**(5), 2009-2019
10. Taylor, K. M. (2000) *IUBMB Life* **49**(4), 249-253
11. Freeman, M. E., Kanyicska, B., Lerant, A., and Nagy, G. (2000) *Physiol Rev* **80**(4), 1523-1631
12. Clevenger, C. V., Chang, W. P., Ngo, W., Pasha, T. L., Montone, K. T., and Tomaszewski, J. E. (1995) *Am J Pathol* **146**(3), 695-705
13. Kelleher, S. L., and Lonnerdal, B. (2005) *Mol Aspects Med* **26**(4-5), 328-339
14. Kelleher, S. L., and Lonnerdal, B. (2005) *Am J Physiol Cell Physiol* **288**(5), C1042-1047
15. Feng, P., Li, T., Guan, Z., Franklin, R. B., and Costello, L. C. (2008) *Mol Cancer* **7**, 25
16. Feng, P., Li, T. L., Guan, Z. X., Franklin, R. B., and Costello, L. C. (2002) *Prostate* **52**(4), 311-318
17. Manning, D. L., Daly, R. J., Lord, P. G., Kelly, K. F., and Green, C. D. (1988) *Mol Cell Endocrinol* **59**(3), 205-212
18. Taylor, K. M., Morgan, H. E., Johnson, A., Hadley, L. J., and Nicholson, R. I. (2003) *Biochem J* **375**(Pt 1), 51-59
19. Kasper, G., Weiser, A. A., Rump, A., Sparbier, K., Dahl, E., Hartmann, A., Wild, P., Schwidetzky, U., Castanos-Velez, E., and Lehmann, K. (2005) *Int J Cancer* **117**(6), 961-973
20. Chowanadisai, W., Kelleher, S. L., and Lonnerdal, B. (2005) *J Nutr* **135**(5), 1002-1007
21. Muylle, F. A., Adriaensen, D., De Coen, W., Timmermans, J. P., and Blust, R. (2006) *Biometals* **19**(4), 437-450
22. Datki, Z. L., Hunya, A., and Penke, B. (2007) *Brain Res Bull* **74**(1-3), 183-187
23. Sensi, S. L., Ton-That, D., Weiss, J. H., Rothe, A., and Gee, K. R. (2003) *Cell Calcium* **34**(3), 281-284
24. Wang, F., Dufner-Beattie, J., Kim, B. E., Petris, M. J., Andrews, G., and Eide, D. J. (2004) *J Biol Chem* **279**(23), 24631-24639
25. Mao, X., Kim, B. E., Wang, F., Eide, D. J., and Petris, M. J. (2007) *J Biol Chem* **282**(10), 6992-7000
26. Dufner-Beattie, J., Kuo, Y. M., Gitschier, J., and Andrews, G. K. (2004) *J Biol Chem* **279**(47), 49082-49090
27. Kim, B. E., Wang, F., Dufner-Beattie, J., Andrews, G. K., Eide, D. J., and Petris, M. J. (2004) *J Biol Chem* **279**(6), 4523-4530
28. Costello, L. C., Franklin, R. B., Liu, Y., and Kennedy, M. C. (2000) *J Inorg Biochem* **78**(2), 161-165

29. Costello, L. C., Liu, Y., Franklin, R. B., and Kennedy, M. C. (1997) *J Biol Chem* **272**(46), 28875-28881
30. Tsui, K. H., Chang, P. L., and Juang, H. H. (2006) *Int J Cancer* **118**(3), 609-615
31. Clegg, M. S., Hanna, L. A., Niles, B. J., Momma, T. Y., and Keen, C. L. (2005) *IUBMB Life* **57**(10), 661-669
32. Chiu, S. M., Xue, L. Y., Usuda, J., Azizuddin, K., and Oleinick, N. L. (2003) *Br J Cancer* **89**(8), 1590-1597
33. Tan, K. O., Fu, N. Y., Sukumaran, S. K., Chan, S. L., Kang, J. H., Poon, K. L., Chen, B. S., and Yu, V. C. (2005) *Proc Natl Acad Sci U S A* **102**(41), 14623-14628
34. Ganju, N., and Eastman, A. (2003) *Cell Death Differ* **10**(6), 652-661
35. Antonsson, B., Montessuit, S., Sanchez, B., and Martinou, J. C. (2001) *J Biol Chem* **276**(15), 11615-11623
36. Shen, H., Qin, H., and Guo, J. (2008) *Mol Biol Rep*
37. Pecina-Slaus, N. (2003) *Cancer Cell Int* **3**(1), 17
38. Christofori, G., and Semb, H. (1999) *Trends Biochem Sci* **24**(2), 73-76
39. Lopez, V., Kelleher, S. L., and Lonnerdal, B. (2008) *Biochem J*
40. Drapier, J. C., and Hibbs, J. B., Jr. (1996) *Methods Enzymol* **269**, 26-36
41. Luetjens, C. M., Kogel, D., Reimertz, C., Dussmann, H., Renz, A., Schulze-Osthoff, K., Nieminen, A. L., Poppe, M., and Prehn, J. H. (2001) *Mol Pharmacol* **60**(5), 1008-1019
42. Kotamraju, S., Konorev, E. A., Joseph, J., and Kalyanaraman, B. (2000) *J Biol Chem* **275**(43), 33585-33592
43. van den Berghe, P. V., Folmer, D. E., Malingre, H. E., van Beurden, E., Klomp, A. E., van de Sluis, B., Merkx, M., Berger, R., and Klomp, L. W. (2007) *Biochem J* **407**(1), 49-59

Appendices

Abstract #1

"Dysregulation of Zip6 (LIV-1) is not potentiated by prolactin in tumorigenic breast cancer cells" Shannon L Kelleher and Veronica Lopez; Era of Hope 2008

Breast cancer is one of the leading causes of death among women. The etiology is unknown; however, compelling evidence implicates dysregulated zinc (Zn) homeostasis in breast cells. Tight regulation of cellular Zn metabolism controls programmed cell death (apoptosis), a process which is uncoupled in cancer. We speculate this is due to dysregulation of Zn transporting mechanisms in breast cells. Zip6 (LIV-1) transports Zn into the cell. Studies in humans have suggested that Zip6 gene expression may be a useful prognostic marker for breast cancer. However, the functional relevance of altered Zip6 expression is not understood.

We hypothesize that alterations in Zip6 dysregulates intracellular Zn pools affecting the ability of cells to undergo apoptosis. To begin to test this hypothesis we measured Zip6 gene expression in cultured tumorigenic (T47D) and normal (HME) human breast cells using quantitative real-time PCR and determined that Zip6 expression was 2-fold lower in tumorigenic cells; similar to what has been reported from breast biopsies. Paradoxically, Zip6 protein abundance was ~10-fold higher. Moreover, in normal breast cells, Zip6 resides almost exclusively on the plasma membrane reflecting its normal role as a Zn import protein. In contrast, ~90% of Zip6 is located intracellularly in tumorigenic breast cells. Confocal microscopy indicated that intracellular Zip6 is restricted to a unique, yet unknown compartment. The identification of this compartment and its role in cellular Zn homeostasis is of critical interest as abnormal protein localization is often linked to metabolic cell disorders. Taken together, this suggests that over-expression and mis-localization of Zip6 protein may play a role in the dysregulation of cellular Zn metabolism and thus contribute to breast cancer pathogenesis.

Recently a relationship between elevated prolactin levels and breast cancer has been observed. Clinical implications reflect the fact that drugs which are widely prescribed for treatment of a range of mental and neurodegenerative illnesses including Parkinson's and depression (e.g. dopamine antagonists) secondarily increase prolactin levels, potentially increasing breast cancer risk in an extraordinary number of individuals. Understanding the relationship between prolactin and breast cancer is of critical importance and may result in novel therapies. We previously determined that prolactin affects Zn metabolism in normal breast cells. Understanding the mechanisms responsible for this regulation and its potential dysregulation in disease is our long-term goal. Thus, we postulate that prolactin plays a regulatory role in Zip6 expression and function. To begin to test this hypothesis we treated tumorigenic breast cells with prolactin and determined that prolactin significantly decreased Zip6 mRNA level (2-fold) while Zip6 protein abundance was concomitantly increased. This suggests that exposure to prolactin may affect breast cell Zn metabolism through further dysregulation of Zip6. We are currently exploring the effects of prolactin in normal breast cells and the functional consequences. In summary, we have begun to examine the role and regulation of Zip6 in tumorigenic breast cells to provide an understanding of its relevance as a potential prognostic marker for breast cancer. Elucidating novel prognostic markers and understanding their role in breast cancer initiation and progression is critical to developing efficacious therapies.

Abstract #2

"Over-expression of Zip6 (LIV1) in tumorigenic breast cancer cells (T47D) cells modulates sub-lethal cytochrome c release and apopotgenesis" Veronica Lopez and Shannon L Kelleher
American Society of Cell Biology 2008

Breast cancer is one of the leading causes of death among women. The etiology is unknown; however, compelling evidence implicates dysregulation of zinc (Zn) homeostasis in breast cancer cells. Humans studies have suggested that over-expression of the zinc importer Zip6 (LIV-1), may be a useful prognostic marker for breast cancer. However, the functional relevance of increased Zip6 expression is not understood. We hypothesize that increased Zip6 expression dysregulates intracellular Zn pools affecting discrete cellular functions, such as apoptosis. Using quantitative real-time PCR, we determined that Zip6 mRNA level was 2-fold lower in tumorigenic breast cells (T47D) compared to normal human breast cells (HME). Conversely, Zip6 protein abundance was significantly higher compared with normal breast cells. Moreover, while Zip6 resided exclusively on the plasma membrane in HMEs reflecting its role as a Zn import protein, ~90% of Zip6 was located intracellularly in T47D cells. To explore the functional role of Zip6 in tumorigenic breast cells, we transfected T47D cells with Zip6 siRNA and examined cytoplasmic Zn levels, vesicular Zn pools and apoptogenesis. Co-transfection of a metal-responsive element (MRE)-luciferase reporter construct in Zip6 attenuated cells significantly reduced cytoplasmic Zn pools in T47D cells. Additionally, Zip6 attenuation significantly reduced vesicular Zn pools as detected with FluorZin-3 AM. To examine affects of diminished cellular Zn pools on cellular function, Zip6 attenuation significantly decreased the sub-lethal release of cytochrome C and subsequently blocked apoptosis by inhibiting caspase-3 and -9 activities. Taken together, this suggests that the tumorigenic potential of T47D cells could be mediated by alterations in intracellular Zn pools via Zip6.

List of personnel supported by this project

Shannon L Kelleher, PhD
Veronica Lopez, PhD

Supporting Data

Table 1: Effect of Zip6 gene suppression on m-aconitase activity in T47D cells.

	Treatment	m-aconitase activity (% of control)	SD
Experiment 1	Control (n=1)	100	N/A
	ZIP6 KO (n=1)	78	N/A
Experiment 2	Control (n=3)	100	2.9
	ZIP6 KO (n=3)	103	3.4

Table 2: Effects of Zip6 gene suppression on caspase activity.

	Activity/µg protein		
	Mock	**Zip6 KO**	**+Zn**
Caspase-1	0.1717 ± 0.01	0.130 ± 0.02*	0.279 ± 0.01*
Caspase-2	0.201 ± 0.01	0.157 ± 0.01*	0.255 ± 0.01*
Capase-3	0.587 ± 0.01	0.448 ± 0.02*	0.683 ± 0.02*
Caspase-9	0.178 ± 0.01	0.142 ± 0.02*	0.301 ± 0.02*

*P<0.01, *t-test analysis of Zip6 suppression (Zip6 KO) and +Zn relative to mock.*

Table 3: Effects of Zip 6 gene suppression on T47D cell colony formation.

	Mock (n=20)	Zip6 KO (n=40)
Mean cell number[1]	18.5 ± 1.1	24.3 ± 1.1*
Number of clusters [2]	25% (5)	43% (17)*

[1] Data represent number of cells/10X magnification field

[2] Data represent % of tumors/10X magnification field (tumors represent clusters of > 3 cells/field); *P<0.001

Table 4: Human and mouse Zip6 primers.

Gene	*Species*	*Forward Primer*	*Reverse Primer*
ZIP6	human	agagccctcccactttgatt	gccgagtgtatcgtggaaat
	mouse	ttcctgtctctgctgggagt	tgtgctgatgacttgcatga
β-actin	human	agaaaatctggcaccacacc	aacggcagaagagagaacca
	mouse	tgttaccaactgggacgaca	ggggtgttgaaggtctcaaa

Table 5: Primers for human Zn transporters.

	Gene	***Forward Primer***	***Reverse Primer***
Zn importers	ZIP1	tcccaaggaacaagagatgg	ctgaaatgggctaggaccaa
	ZIP3	gtgggcgtgttcttcttcat	ctggagctttccctcacag
	ZIP8	tcctgcaccttgtctctcct	gcccaacatagcaggaacat
	ZIP10	cctttgccctgcattgttat	agatcacgcctagcaaggaa
Zn exporters	ZnT1	cgcacttggctgtctttaca	ctttggcagagcaaggtttc
	ZnT2	tgcccagttatcagggagtc	gccaactggctcttgttctc
	ZnT4	tctgggtgtgaacgtaacca	gatggggtcagcaatcttgt
Other	E-cadherin	tgcccagaaaatgaaaaagg	ggatgacacagcgtgagaga

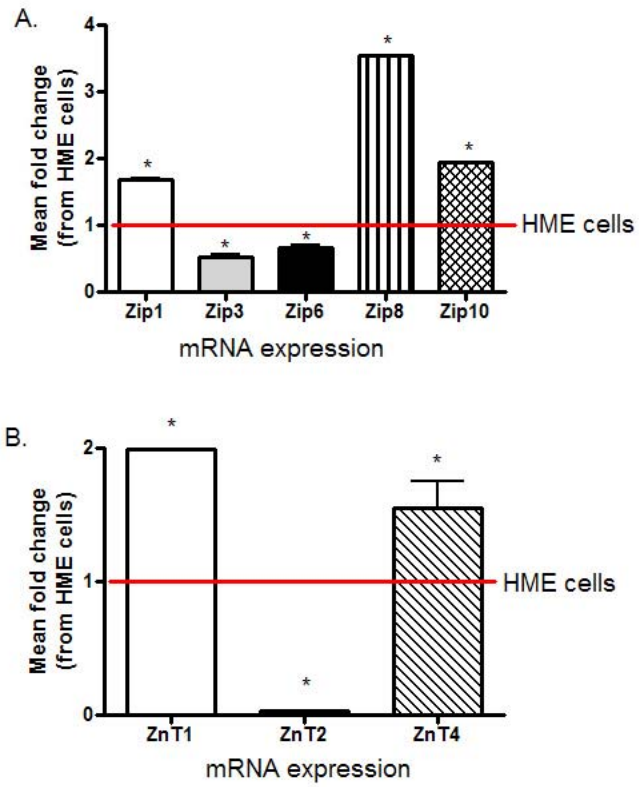

FIGURE 1: Differential mRNA expression of Zn transporters in breast cells. Q-PCR was used to compare mRNA levels between tumorgenic (T47D) and normal HME cells (red line). (A) Expression of Zn importers (Zip) Zip1,-8 and -10 were elevated several fold, while expression of Zip3 and -6 were significantly lower in T47D cells compared to that observed in HME cells (red line). (B) Evaluation of Zn importers (ZnT) revealed that ZnT1 and -4 mRNA were abundantly expressed, whereas ZnT2 expression was barely detected in T47D cells compared with HME cells. Data represent mean fold-change from HME cells set at 1 (n=3 samples per group ± standard deviation).

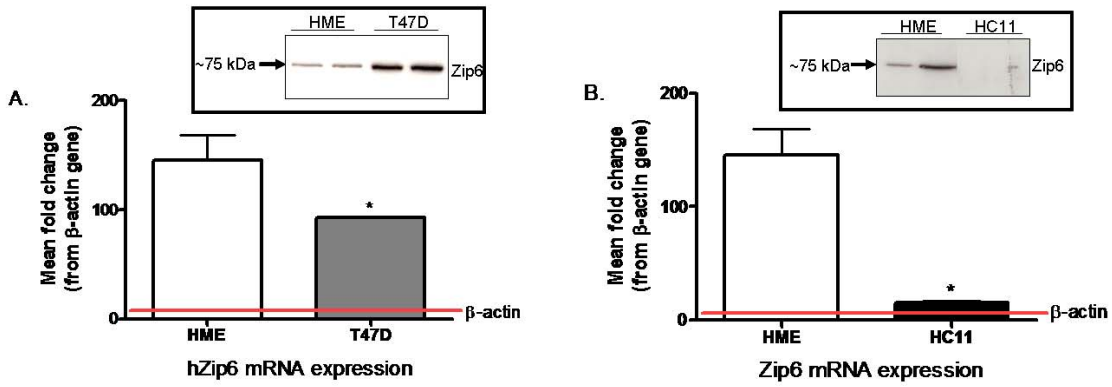

FIGURE 2: Endogenous Zip6 expression in human (HME and T47D) and mouse (HC11) breast cells. Q-PCR and immunoblotting was used to compare Zip6 expression between HME cells and T47D cells (A) and between HME and HC11 cells (B). (A) Both HME and T47D cells expressed Zip6 mRNA, however Zip6 expression was significantly lower in T47D cells compared to HME cells. Conversely, Zip6 protein abundance was ~10-fold higher in T47D cells compared to HME cells (inset). (B) HME and HC11 cells expressed Zip6 mRNA although HC11 cells expressed relatively minimal amounts of Zip6 compared with HME cells. No detectable Zip6 protein was observed in HC11 cells (inset). Data represent mean fold change from β-actin set at 1 (n=3 samples per group ± standard deviation; asterisk, $P<0.005$).

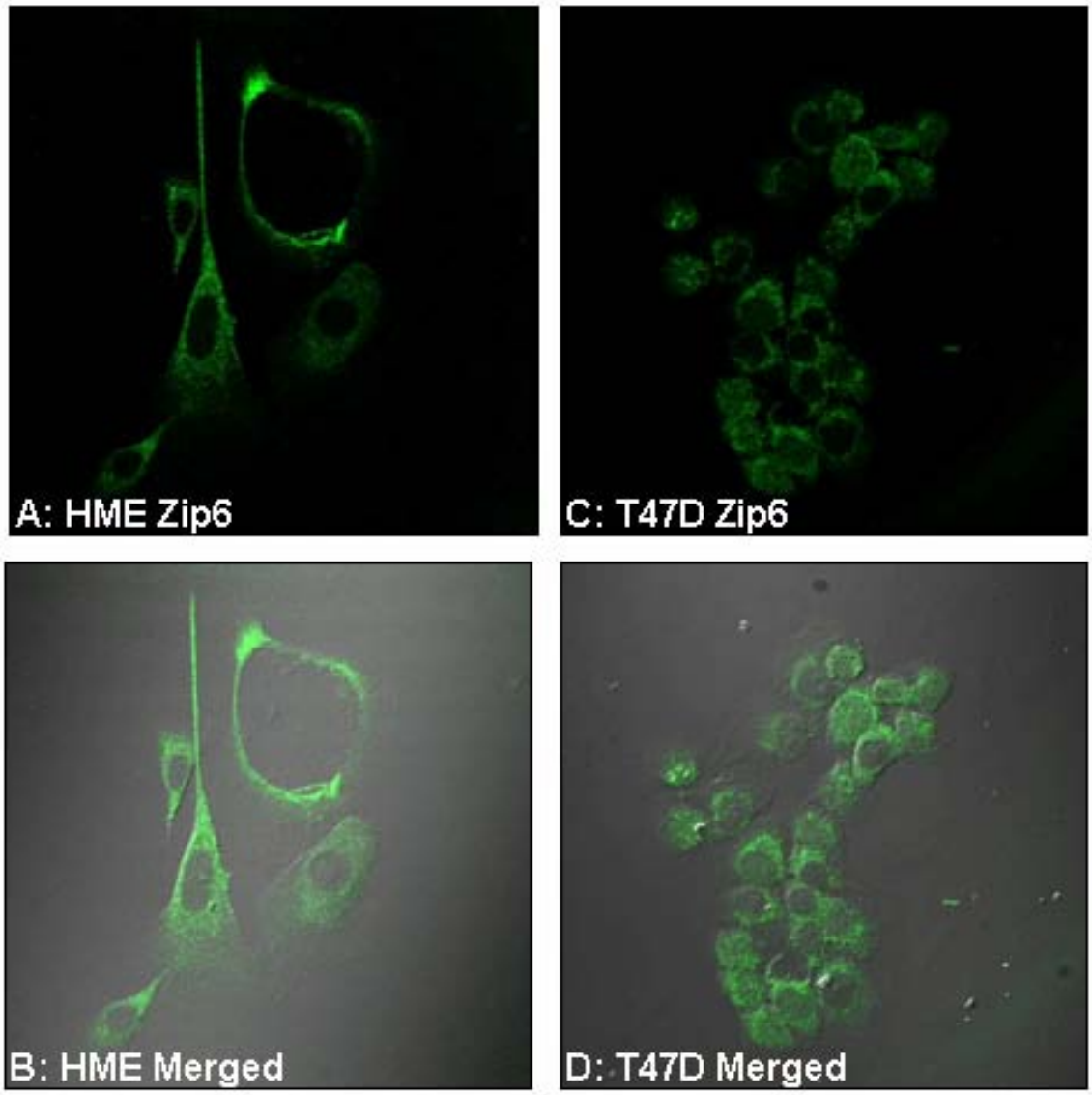

FIGURE 3: Exofacial localization of endogenous Zip6 by confocal microscopy in HME and T47D cells. Cells were fixed in paraformaldehyde, not permeabilized (without 0.2% Triton X-100), and incubated with anti-Zip6 antibody. Zip6 protein was detected with rabbit IgG conjugated to Alexa 488. (A-B) A consistent diffuse staining pattern was observed in HME (A-B) and T47D (B-D) cells. However, HME cells routinely illustrated specific regions of slightly more intense Zip6 staining compared to T47D cells. Images collected at 60X magnification, under oil.

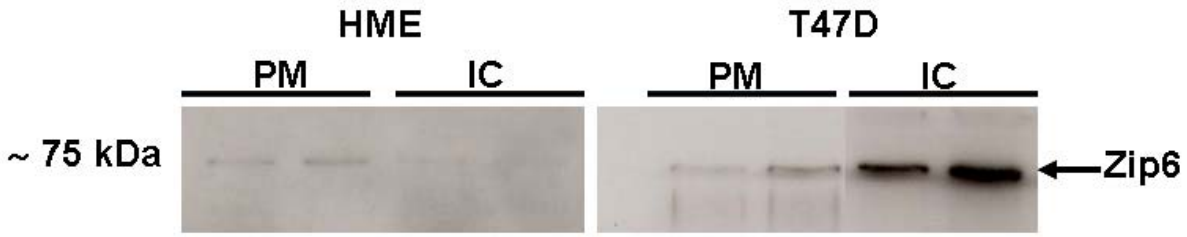

FIGURE 4: Cell surface biontinylation of endogenous Zip6 in HME and T47D cells. Plasma (PM) and intracellular (IC) membrane fractions were isolated, separated by electrophoresis and Zip6 abundance was compared by immunoblotting. Consistent with previous data, Zip6 was plasma membrane-associated in both HME and T47D cells, however T47D cells contained a large fraction of intracellular (IC) membrane-associated Zip6 compared with that observed in HME cells.

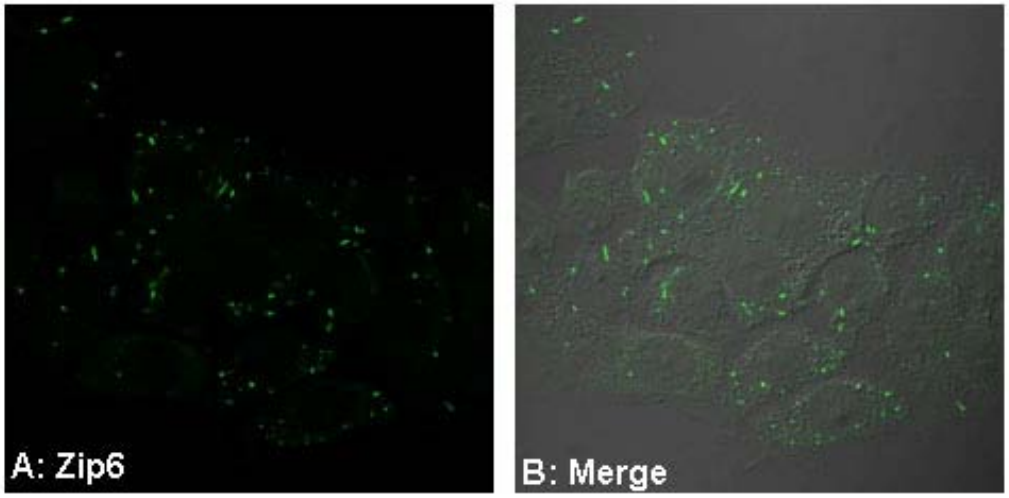

FIGURE 5: Endogenous localization of Zip6 in T47D cells by immunofluorsence. Cells were fixed in paraformaldehyde, permeabilized (0.2% Triton X-100), and then incubated with anti-Zip6 antibody. Zip6 protein was detected with rabbit IgG conjugated to Alexa 488. (A) Immunofluorescence revealed Zip6 localized in a rod-like pattern. (B) The overlay of Zip6 demonstrated the cytoplasmic localization of the punctate spindle-like forms. Images collected at 60X magnification, under oil.

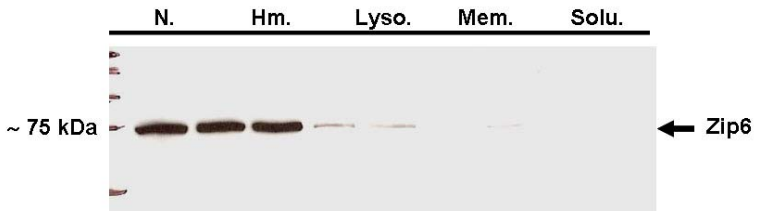

FIGURE 6: Localization of endogenous Zip6 by differential centrifugation in T47D cells. Total cellular homogenate was subjected to differential centrifugation for cellular organelle density fractionation and fractions were analyzed by immunoblotting for Zip6. The majority of Zip6 was localized in fractions enriched in nuclei (N) and heavy mitochondria (Hm), with minor amounts associated with the lysosomal (Lyso) and endosomal membrane (Mem) fractions. As expected, Zip6 was absent from the cytoplasmic (Solu) fraction, suggesting Zip6 is localized in a very dense cellular compartment.

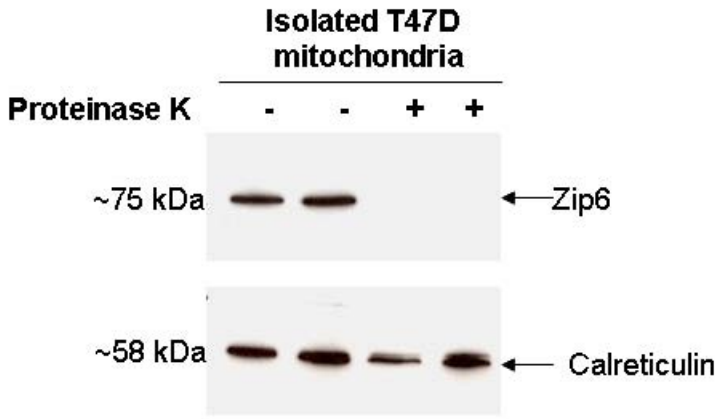

FIGURE 7: Endogenous Zip6 is absent from the mitochondria in T47D cells. Isolated mitochondria were incubated without (-) and with (+) proteinase K to attempt eliminate endoplasmic reticulum surrounding the mitochondria. Immunoblotting revealed Zip6 in untreated crude mitochondria fractions, while proteinase K treatment clearly eliminated Zip6 detection. These data indicate that Zip6 is not localized to mitochondria but was instead a component of a contaminating membrane fraction. Membrane was then stripped and reprobed with calreticulin, a maker for endoplasmic reticulum, which was observed in untreated cells however, the addition of proteinase K reduced the amount of calreticulin detected.

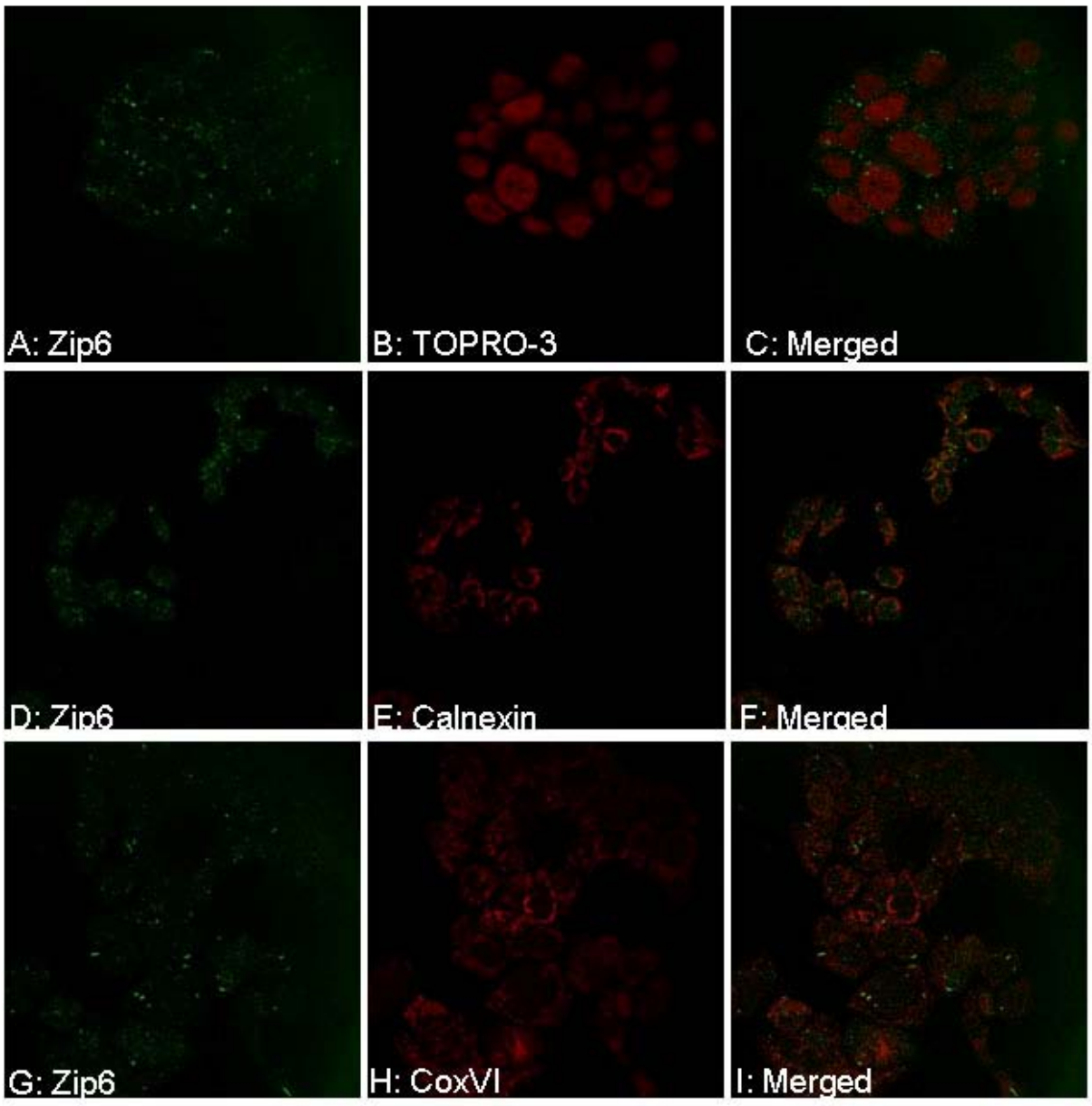

FIGURE 8: Endogenous sub-cellular localization of Zip6 in tumorigenic T47D cells. Images represent confocal microscopy illustrating Zip6 (green) stains in a punctate spindle-like pattern promixal to the nucleus (TOPRO, red) in T47D cells (A-C). Double immunofluorescence imaging of Zip6 (green, D) and calnexin (endoplasmic reticulum marker, red; E) and cytochrome c oxidase subunit IV (CoxIV, mitochondrial marker, red; H) illustrates no co-localization (merge, yellow; F and I) between Zip6 and endoplasmic recticulum or mitochondria. Images collected at 60X magnification, under oil.

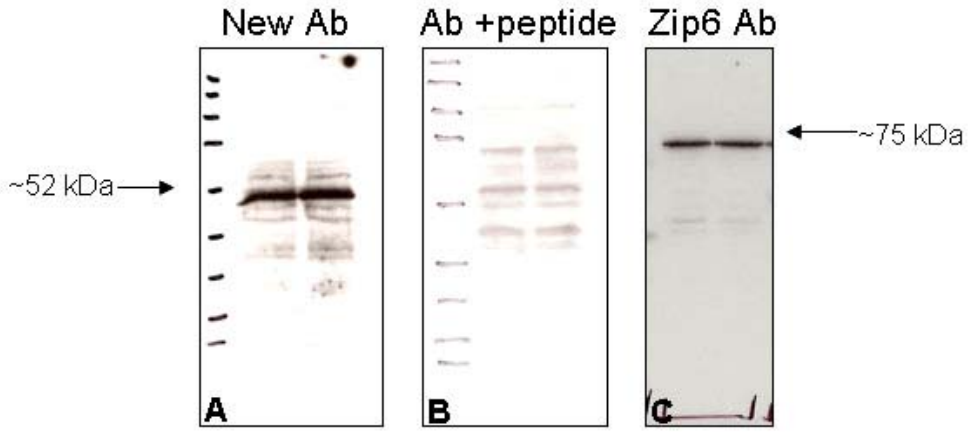

FIGURE 9: Characterization of Zip6 antibody. Crude membrane fractions were isolated from T47D cells and protein (50 μg) was electrophoresized to identify immunoreactive Zip6 proteins. (A) Our new Zip6 antibody (New Ab) clearly revealed a major band at ~50 kDa, which was completely eliminated by peptide competition (B). In contrast, the antibody provided by Dr. Huang (Zip6 Ab) detected a single band at ~75 kDa (C), similar to previous reports.

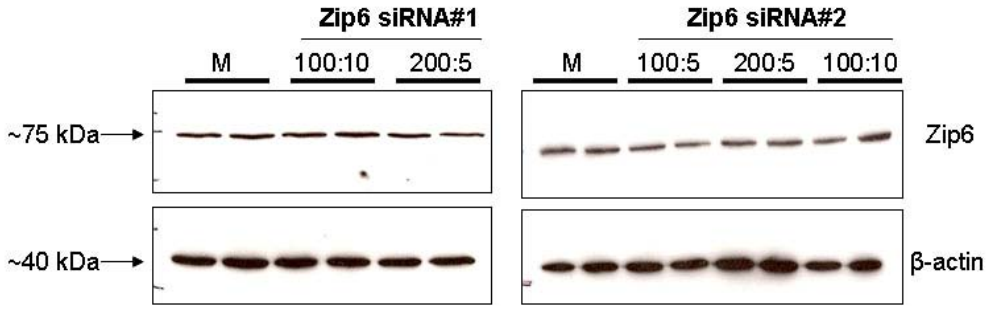

Figure 10: Zip6 gene knockdown with Lipofectamine 2000 in T47D cells. Cells were seeded in antibiotic-free Opti-MEM medium (Invitrogen) in 6-well plates and cultured until ~50% confluent. Cells were transiently transfected with specific Zip6 siRNA #1 at a DNA: transfection reagent ratio according to manufacturer's specifications; 100 pmol: 10 μL Lipofectamine 2000 (100:10), 200 pmol: 5 μL (200:5) or Zip6 siRNA #2 at 100 pmol: 5 μL Lipofectamine 2000 (100:5), 200 pmol: 5 μL (200:5), 100 pmol: 10 μL (100:10), in antibiotic-free Opti-MEM medium for 24 h. Total crude membranes were isolated and immunoblotted for Zip6. Attempted optimization of gene suppression did not reveal significant knockdown of Zip6 in cells treated with siRNA compared to non-treated mock (M) controls, as anticipated. β-actin was used as a loading control.

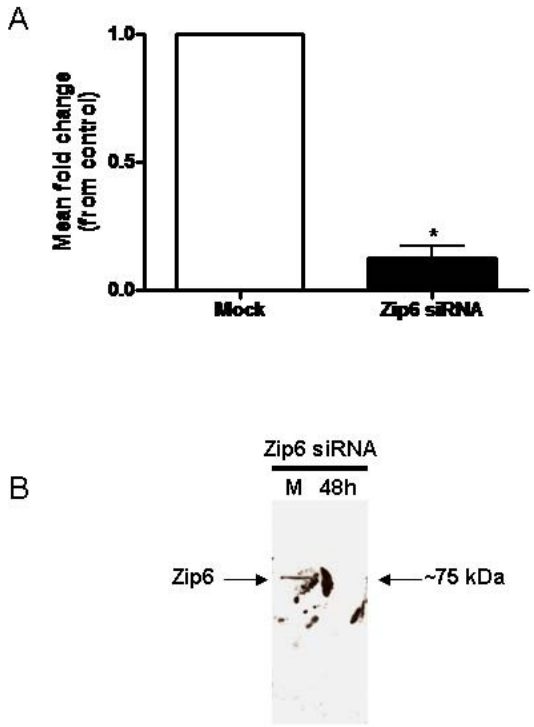

Figure 11: Zip6 gene suppression with Amaxa Nucleofactor System in T47D cells. Cells were transfected in antibiotic-free medium with 200 pmol of Zip6 siRNA and cultured for 48 h per manufacture's recommendations. Cells were collected and analyzed for mRNA and protein expression. (A) By Q-PCR, we demonstrated that Zip6 expression was significantly reduced when compared to mock transfected cells (M) after 48 h. (*$P<0.05$) (B) Concomitantly, Zip6 protein was also significantly reduced compared to mock transfected cells (M).

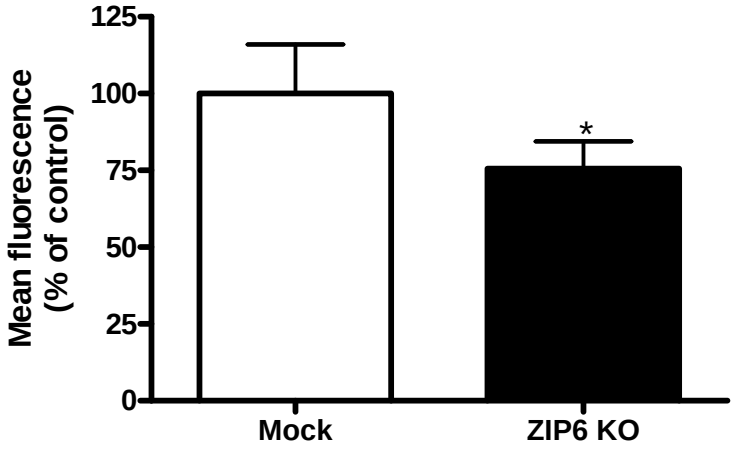

Figure 12: Cellular Zn accumulation was reduced with Zip6 gene suppression in T47D cells. Zinc accumulation was measured using FluorZin-3 fluorescence in cells transfected with Zip6 siRNA (ZIP6 KO) and compared with mock-transfected cells (Mock) measured as arbitrary fluorescence units/μg protein. Zip6 gene attenuation significantly reduced Zn accumulation compared to mock transfected cells. Data represent mean % fluorescence relative to mock-transfected control cells ± standard deviation (n=6-8 samples/group). Asterisk represents a significant effect of gene suppression, $p<0.05$.

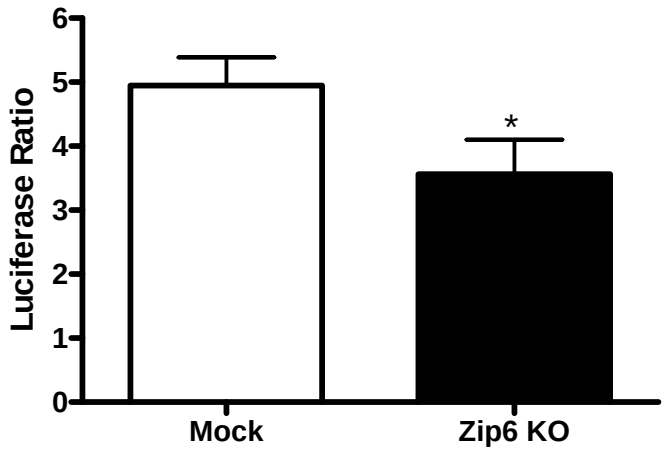

Figure 13: Zip6 gene attenuation reduced cytoplasmic Zn pools in T47D cells. Cytoplasmic Zn level was measured using a 4X-Metal-response element (MRE) luciferase reporter construct in cells treated with Zip6 siRNA (Zip6 KO) and compared with mock-transfected cells (Mock). Zip6 gene attenuation significantly reduced luminescence suggesting that cytoplasmic Zn pools were lower compared to mock transfected cells. Data represent ratio of firefly:renilla luciferase activity ± standard deviation (n=3 samples/group). Asterisk represents a significant effect of gene suppression, $p<0.05$.

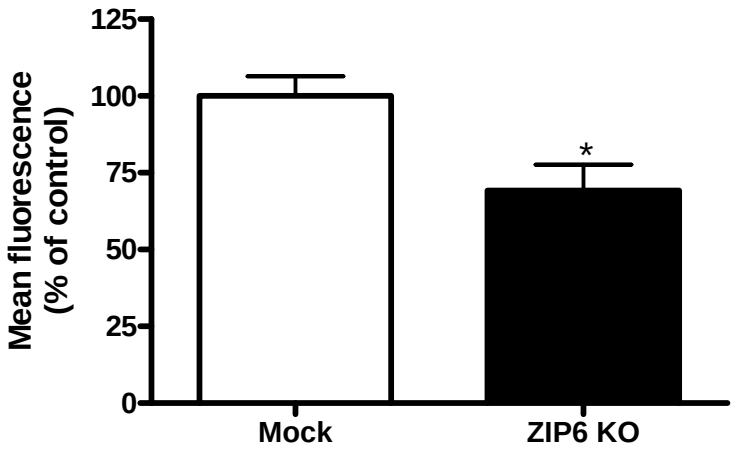

Figure 14: Mitochondria Zn pools were reduced with Zip6 gene suppression in T47D cells. Mitochondria Zn accumulation was measured using Rhodzin-3 fluorescence in cells transfected with Zip6 siRNA (ZIP6 KO) and compared with mock-transfected cells (Mock) measured as arbitrary fluorescence units/μg protein. Zip6 gene attenuation significantly reduced RhodZin-3 fluorescence suggesting that mitochondria Zn accumulation was lower compared with monck-transfected controls. Data represent mean % fluorescence relative to mock-transfected cells ± standard deviation (n=6-8 samples/group). Asterisk represents a significant effect of gene suppression, $p<0.05$.

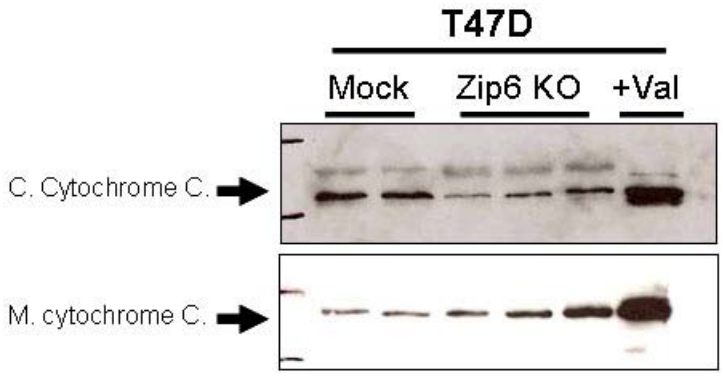

Figure 15: Zip6 gene attenuation inhibited cytochrome C release in T47D cells. Cytoplasmic release of cytochrome C was measured in cells transfected with Zip6 siRNA (Zip6 KO) and compared to mock-transfected cells (Mock). Total cytoplasmic (C) and mitochondria (M) fractions were isolated and immunoblotted. Zip6 gene suppression significantly reduced cytochrome C release when compared to mock-transfected controls. To validate our assay of mitochondria release of cytochrome C in T47D cells, valinomycin was used as a positive control as it has been shown to induce apoptosis via mitochondria permeability.

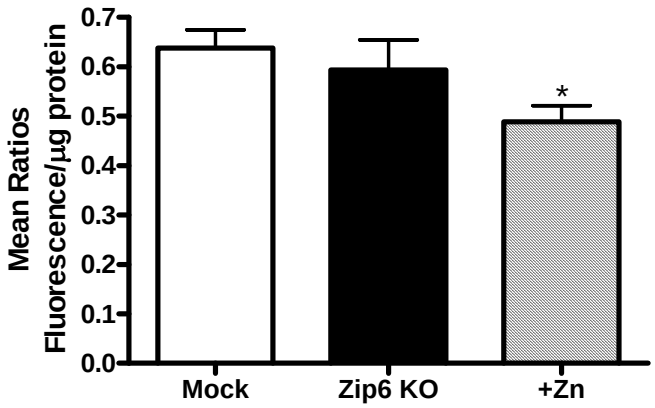

Figure 16: Alterations in mitochondrial membrane potential were not affected by Zip6 gene attenuation in T47D cells. Mitochondrial membrane potential was measured using JC-1 fluorescence in cells treated with Zip6 siRNA (Zip6 KO) and compared with mock-transfected cells (Mock) measured as arbitrary fluorescence units/μg protein. Zip6 gene suppression did not significantly affect mitochondria potential compared to controls; however, the addition of Zn (75 μM) for 4 h significantly reduced mitochondrial membrane potential validating our assay. Data represent mean ratios of red:green fluorescence ± standard deviation (n=6-8 samples/group). Asterisk represents a significant effect of Zn treatment, $p<0.05$.

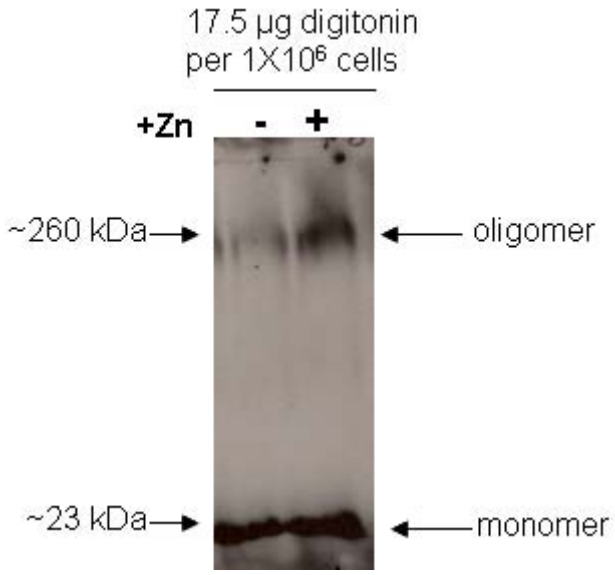

Figure 17: Zinc induced bax oligomerization in T47D cells. Cells were incubated with Zn (75 µM) for 4 h. Total cell lysates were isolated and incubated with digitonin, then crosslinked with glutaraldehyde (0.3%) and subsequently analyzed for Bax oligomers by immunoblotting. Inherent Bax oligomerization (260 kDa) was observed in the absence of Zn; however, the addition of Zn significantly increased abundance of Bax oligomerization in cells, implicating decreased mitochondria potential.

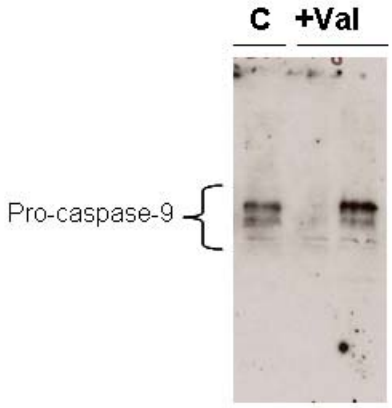

Figure 18: Constitutive amounts of activated caspase-9 were undetected in T47D cells. Cells were treated with a known mitochondrial membrane disruptor, valinomycin (Val) for 24 h and compared wth non-treated cells. Total cell lysates were collected and proteins (50 μg) were immunoblotted with anti-caspase-9 antibody. The expected presence of cleaved caspase-9 (~38 and ~17 kDa) fragments was not observed in cells untreated and Val treated cells.

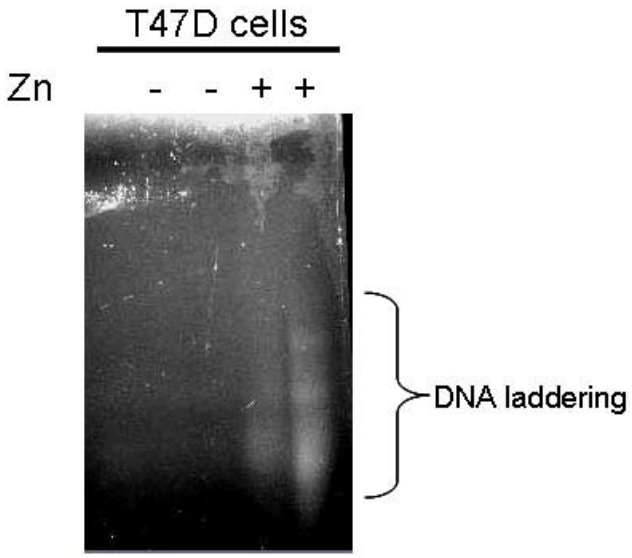

Figure 19: Zn induced DNA fragmentation in T47D cells. Cells were incubated with Zn (75 μM) for 24 h and DNA fragmentation (180-200 bp) was measured by ethidium bromide staining of DNA electrophoresed through agarose gels. The expected DNA laddering was observed in cells treated with Zn compared to untreated cells. However, no basal amounts of DNA laddering were detected in untreated cells as anticipated.

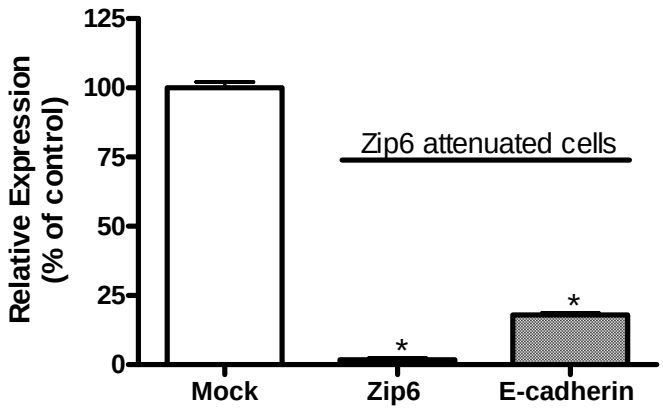

Figure 20: E-cadherin mRNA expression is positively associated Zip6 gene attenuation in T47D cells. E-cadherin expression was measured by Q-PCR in cells treated with Zip6 siRNA (Zip6) and compared with mock-transfected cells (Mock). Zip6 gene suppression resulted in a significantly reduction in E-cadherin expression, suggesting changes in cell phenotype. Data represent mean ± standard deviation (n=3 samples/group). Asterisk represents a significant effect of gene suppression, $p<0.05$.

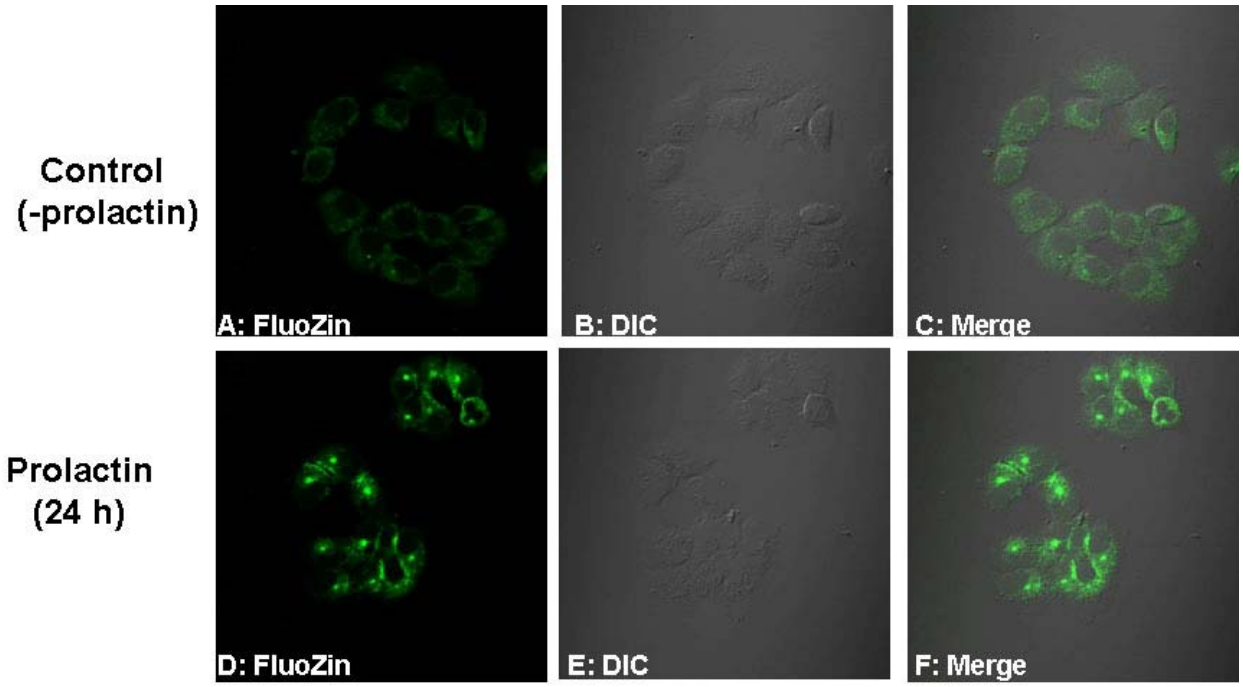

Figure 21: Intracellular Zn pools are increased in response to prolactin (PRL) in T47D cells. Zinc accumulation was visualized by immunofluorescence using FluoZin-3 in cells treated with PRL (D-F) and compared with untreated cells (A-C). Prolactin significantly increased well-defined cellular Zn pools (D-F), compared to untreated cells (A-C). Additionally, untreated cells demonstrated dispersed Zn pools (A-C). Images collected at 60X magnification, under oil.

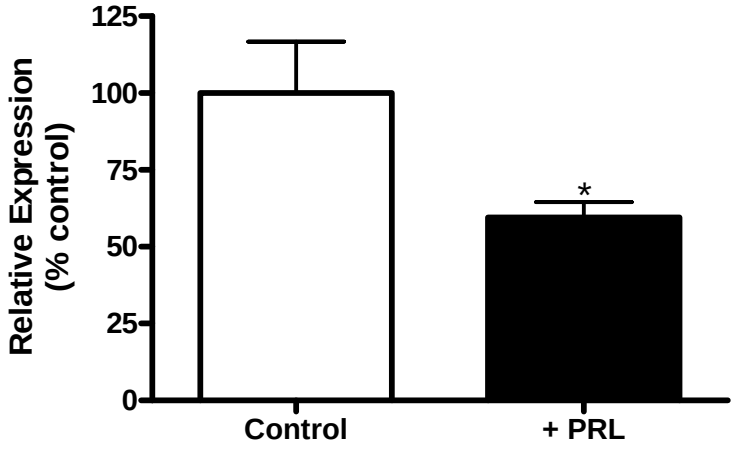

Figure 22: Zip6 mRNA expression is negatively regulated by prolactin (PRL). Zip6 expression was measured by Q-PCR in cells treated with PRL (+PRL) and compared with untreated control cells (Control). The addition of PRL significantly reduced Zip6 expression. Data represent mean ± standard deviation (n=3 samples/group). Asterisk represents a significant effect of PRL, $p<0.05$.

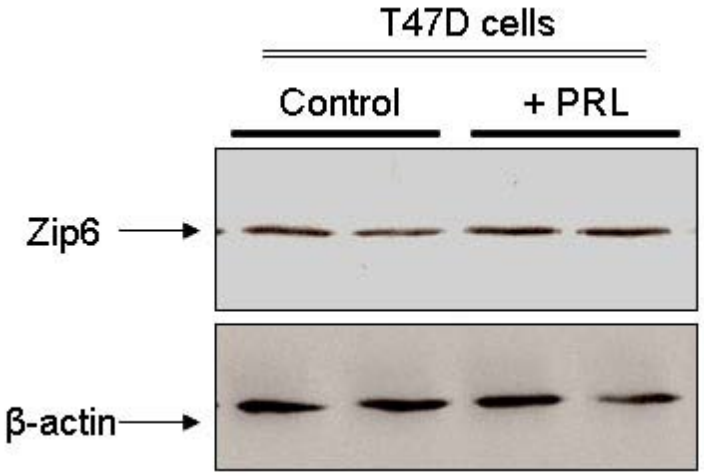

Figure 23: Zip6 protein abundance is minimally affected by PRL in T47D cells. Cells were treated with PRL (+PRL) and compared to non-treated cells (Control). Crude membrane fractions were isolated and immunoblotted for Zip6. A robust affect of PRL on Zip6 protein abundance was not observed in PRL-treated cells compared with non-treated cells, suggesting that PRL plays a minimal role in Zip6 protein expression. β-actin was used as a loading control.

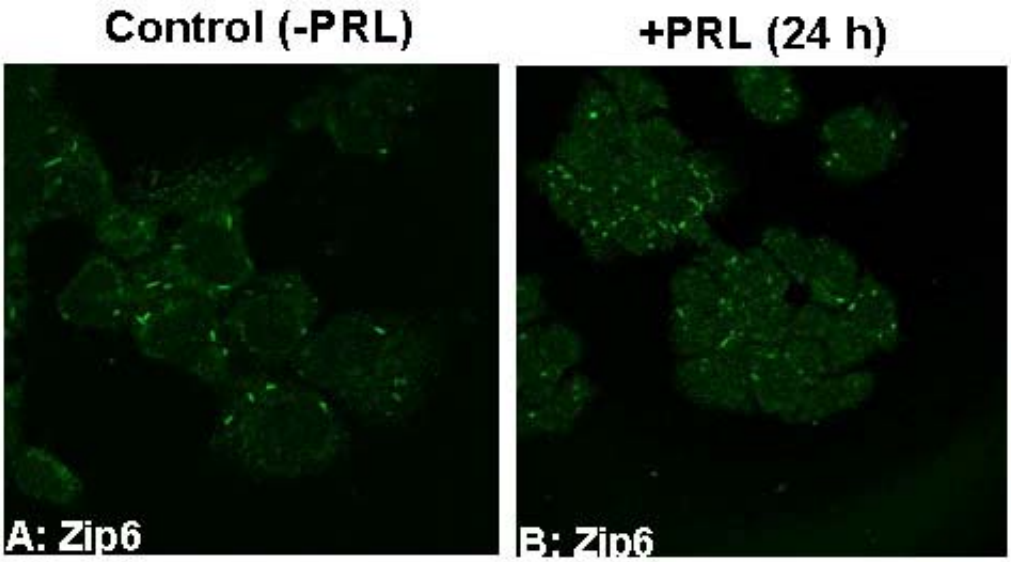

Figure 24: Localization of Zip6 is not potentiated by PRL in T47D cells. Changes in Zip6 localization were visualized by immunofluorescence in cells treated with PRL (B) and compared with untreated control cells (A) as previously described. Cells were fixed in paraformaldehyde, permeabilized and then incubated with anti-Zip6 antibody. Zip6 was detected with rabbit IgG conjugated to Alexa 488. Immunofluorescence revealed Zip6 localized in a rod-like pattern in untreated cells (A) which was not significantly altered in the presence of PRL (B), suggesting that PRL does mediate Zip6 re-localization in T47D cells. Images collected at 60X magnification, under oil.